To the Graduate Council:

I am submitting herewith a thesis written by Xinlei Wang entitled "A New High-speed Simulation Method for Electron Beam Microanalysis". I have examined the final copy of this thesis for form and content and recommend that it be accepted in partial fulfillment of the requirements for the degree of Master of Science, with a major in Metallurgical Engineering.

David C Joy

David C. Joy, Major Professor

We have read this thesis
and recommend its acceptance:

Charlie R. Brooks

Thomas L. Mock

Accepted for the Council:

Lee Minkel

Associate Vice Chancellor
and Dean of The Graduate School

STATEMENT OF PERMISSION TO USE

In presenting this thesis in partial fulfillment of the requirements for a Master's degree at The University of Tennessee, Knoxville, I agree that the Library shall make it available to borrowers under rules of the Library. Brief quotations from this thesis are allowable without special permission, provided that accurate acknowledgment of the source is made.

Permission for extensive quotation from of reproduction of this thesis may be granted by my major professor, or in his absence, by the Head of Interlibrary Services when, in the opinion of either, the proposed use of the material is for scholarly purposes. Any copying or use of the material in this thesis for financial gain shall not be allowed without my written permission.

Signature Xinlei Wang

Date July 29, 1992

Requests for permission for extensive quotation from or reproduction of this thesis in whole or in parts may be granted by the copyright holder.

A New High-speed Simulation Method for Electron Beam Microanalysis

A Thesis
Presented for the
Master of Science
Degree
The University of Tennessee, Knoxville

Xinlei Wang
August, 1992

Copyright © Xinlei Wang, 1992

All rights reserved

DEDICATION

This thesis is dedicated to my parents

Mr. Kai Wang

&

Mrs. Yongjie Kim

Acknowledgments

I would like to express my sincere gratitude to my major professor, Dr. David C. Joy, for his concern, guidance, patience, encouragement and financial support throughout the course of this research. I would also like to thank my other committee members, Dr. Charlie R. Brooks and Dr. Thomas T. Meek for their friendly advice and consultation.

Thanks also goes to Dr. John Dunlap, Mr. Richard Williams and Dr. Carolyn Joy for their assistance with the experiment, to Mrs. Suichu Luo for her contributive comments during the study, to Dr. Zibby Czyzewski for his helpful discussions, and to Mrs. Jennifer Trollinger for her help and support.

The author is indebted to all the professors and her fellow graduate students in the Department of Materials and Engineering for their generous support and encouragement in the pursuit of this degree.

ABSTRACT

The BSE, SE, x-ray signals produced from a bulk specimen have been successfully studied with a high degree of accuracy by the Monte Carlo technique. However, such procedure takes considerable computing time since any change of experimental parameters requires a fresh computation. This thesis describes an alternative approach that permits the BSE, SE yield and EDS spectrum of a given structure to be computed within a fraction of a second. The procedure used is called the diffusion matrix model.

At first, a Monte Carlo simulation is described in detail in the thesis. The diffusion matrix method is then developed by a simple Monte Carlo computation, and used to collect the yield of BSE, SE signal and the intensity of bremsstrahlung and characteristic x-rays. At last, the BSE, SE, and x-ray signals from a surface of a given geometry can be found by simple summation of the matrix, and the results of any change in the geometry can be determined immediately without the need of a new set of a Monte Carlo simulation. The agreement of the theoretical and experimental results indicates the practical approach of the diffusion matrix model. Such a procedure has the advantage of its application to the micro-particles, arbitrary topography, heterogeneous sample, and multi-layer specimens.

TABLE OF CONTENTS

CHAPTER PAGE

1. MONTE CARLO MODELING AND TRANSPORT THEORY.....1

1-1. The Single Scattering Monte Carlo Model.....2

1-2. The Plural Scattering Monte Carlo Model.....7

2. DIFFUSION MATRIX MODEL.....12

2-1. Introduction.....12

2-2. The Development of the Diffusion Matrix Model for SE and BSE Signals....13

2-3. The Extension of the Diffusion Matrix Model to X-ray Generations.....16

2-4. Calculation of a Signal Profile.....25

3. THE APPLICATION OF THE MATRIX MODEL.....39

3-1. To Examine BSE, SE Signals on an Edge Inclination Topography.....39

3-2. EDS Spectrum for Rough Materials.....42

3-3. The Use of the Background Radiation in Electron Probe Micro-analysis of Bulk Samples.....44

3-4. Properties of Characteristic-to-Bremsstrahlung Ratios 45

4. THE FURTHER APPLICATION OF THE MATRIX MODEL TO HETEROGENEOUS SPECIMEN.....46

4-1. EDS Spectrum Simulation for a System with More Than One Component...46

4-2. EDS Spectrum Evaluation for a Multi-layer Sample.....48

5. SUMMARY.....52

5-1. Discussion.....52

5-2. Conclusion.....53

LIST OF REFERENCES.....54

APPENDIX.....58
VITA.....74

LIST OF FIGURES

FIGURE PAGE

1. Schematic of Monte Carlo simulation....3
2. Flow chart for single scattering Monte Carlo model....8
3. Flow chart for plural scattering Monte Carlo model....11
4. The schematic geometry of the diffusion matrix....14
5. Schematic diagram of geometrical relationships between the observation direction and electron direction for any single trajectory....20
6. Schematic illustration of method to calculate a BSE, SE signal profile for a given geometry structure from the diffusion matrix....26
7. Schematic illustration of diffusion matrix applied to a round topography sample for the simulation of bremsstrahlung x-ray intensity....27
8. Comparison of EDS spectrum (I) measured at SEM-800, (II) calculated by diffusion matrix method....30
9. Comparison of BSE signals from detector A and B for silicon specimen at 2.0keV....40
10. Comparison of BSE and SE Signals by matrix model to that by Monte Carlo simulation on a silicon structure....41
11. Diffusion matrix calculation of bremsstrahlung x-ray for a round Al particle at 20 keV 42
12. Diffusion matrix calculation of bremsstrahlung x-ray on a wave shaped surface of Al specimen at 20 keV....43
13. Log plot of the integral of background radiation to atomic number....44
14. EDS Spectrum of Fe-Ni Alloy at E0=20keV (a) from the experimental data b) from the calculation by diffusion matrix method....47

15. Schematic illustration of the application of matrix method to multi-layer film specimen.....49
16. EDS Spectrum of Cu/Cr two-layer sample with t_{Cu}=5208Å at E0=20keV.....51

CHAPTER 1

MONTE CARLO MODELING AND TRANSPORT THEORY

The interaction of an electron beam with a solid can be modeled by the so-called Monte Carlo method. This technique produces a stepwise simulation of the electron trajectory by using random numbers to predict scattering angles on the basis of theoretical probability distributions or empirical models (Joy 1991). Each incident electron is traced during its many collisions to obtain all the necessary information, such as backscattered, secondary yield, and x-ray generation, etc., until it loses its energy or escapes from the specimen. Such a procedure is quite powerful in the study of the characteristics and distributions of the various signals generated in electron-specimen interactions.

Before considering the different Monte Carlo approaches that have been used, it is instructive to give two significant assumptions in discussing the interaction between the electron beam and solid.

1) Only elastic scattering events are considered in producing significant angular deviation when the electron interacts with the solid. Elastic scattering, described by the screened Rutherford cross-section and produced by coulombic attraction between the negatively charged electron and a positively charged nucleus, results in angular deflections of from a few degrees up to 180°. The great majority of inelastic scattering events produces angular deflections which are typically 1/2° or less. Consequently elastic scattering events dominate in determining the spatial distribution of the interaction.

2). The energy loss due to inelastic scattering is assumed by means of the Bethe continuous energy loss relation (1930), rather than as a result of a discrete inelastic event. This approximation allows the net results of all possible inelastic scattering processes to be accounted for in a simple expression.

1-1. The Single Scattering Monte Carlo Model

The coordinate system in the simulation of the electron trajectories is set as follows: The positive z-axis is set to be the same as the direction of the incident beam, the x-axis lies on the specimen surface and vertical to the beam direction, and y-axis completes a right handed set of axes. Assume the electron undergoes an elastic scattering event at the point P_n (x,y,z), which is originally from P_{n-1}, to the point $P_{n+1}(x_n,y_n,z_n)$. To obtain the new coordinate of point P_{n+1}, we need to first calculate the step length between the subsequent scattering and the elastic scattering angle ϕ and Ψ. The schematic of Monte Carlo simulation is shown in figure 1.

The relativistically corrected screened Rutherford elastic cross-section σ_E is given by the relation

$$\sigma_E = 5.21\times10^{-21}\cdot\frac{Z^2}{E^2}\cdot\frac{4\pi}{\alpha(1+\alpha)}\cdot\left(\frac{E+511}{E+1024}\right)^2(cm^2) \qquad (1.1)$$

where E is the electron energy (in keV), Z is the atomic number of the target, and α is a screening factor which accounts for the fact that the incident electron does not see all of the charge on the nucleus because of the orbiting electrons and is found by Bishop (1976)

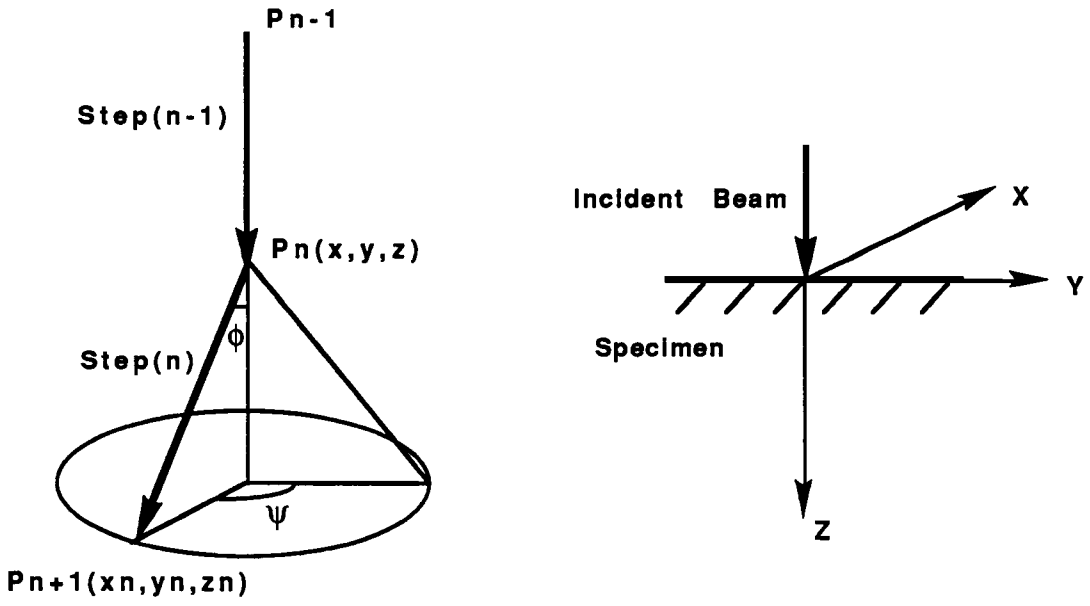

Figure 1. Schematic of Monte Carlo simulation. The electron travels from a known point P_n to an unknown point P_{n+1}. The right side graph shows its coordinate system.

$$\alpha = 3.4 \times 10^{-3} \cdot \frac{Z^{0.67}}{E} \tag{1.2}$$

The elastic cross-section defines a mean free path λ which is given by the formula

$$\lambda = \frac{A}{N_a \rho \sigma_E}(cm) \tag{1.3}$$

where N_a is Avogadro's number, ρ is the density (in gm/cm^3) and A is the atomic weight (in gm/mole). λ describes the average distance that an electron will travel between encountering elastic scattering events. Since the real path is distributed about the mean, a distribution is applied to calculate the step length by the equation as follows

$$step = -\lambda \cdot \log_e(RND)(cm) \tag{1.4}$$

where RND is a linearly distributed random number between 0 and 1.

The scattering angular deviation is determined by $d\sigma_E / d\Omega = \sigma'$, so

$$RND = \int_0^{\phi} \frac{\sigma'}{\sigma_E} d\Omega \tag{1.5}$$

The right hand side of equation (1.5) represents the probability of the electron being scattered through an angle less than ϕ. By evaluating equation (1.5), the equation can be derived (Newbury et al. 1976) which relates the scattering angle ϕ to the random number RND

$$\cos(\phi) = 1 - \frac{2\alpha \cdot RND}{(1 + \alpha - RND)} \tag{1.6}$$

where α is the screening coefficient given above. This equation generates a unique scattering angle in the range $0 < \phi < 180°$ with the great majority of scattering angles in the range from 0 to 10°.

The azimuthal scattering angle in the base of the cone shown in figure 1 can take on any value in the range of 0 to 360°, so that this angle, Ψ, is chosen by the equation, with another choice of random number R, 0 <= R <= 1

$$\Psi = 2\pi \cdot RND \tag{1.7}$$

The new coordinate (x_n, y_n, z_n) is then obtained by Newbury et al. (1976) relative to the previous point (x,y,z):

$$x_n = x + step \cdot ca \tag{1.8a}$$

$$y_n = y + step \cdot cb \tag{1.8b}$$

$$z_n = z + step \cdot cc \tag{1.8c}$$

where

$$ca = (cx \cdot \cos\phi) + (V1 \cdot V3) + (cy \cdot V2 \cdot V4) \tag{1.9a}$$

$$cb = (cy \cdot \cos\phi) + (V4 \cdot (cz \cdot V1 - cx \cdot V2)) \tag{1.9b}$$

$$cc = (cz \cdot \cos\phi) + (V1 \cdot V3) - (cy \cdot V1 \cdot V4) \tag{1.9c}$$

and

$$V1 = AN \cdot \sin\phi,$$

$$V2 = AN \cdot AM \cdot \sin\phi$$

$$V3 = \cos\Psi$$

$$V4 = \sin\Psi \qquad (1.10a)$$

where

$$AM = -\frac{cx}{cz}, and, AN = \frac{1}{\sqrt{1+AM^2}} \qquad (1.10b)$$

The electron energy loss equation (stopping power expression) is given by the modified Bethe equation which is good down to energies of 100 eV or below (Joy and Luo 1989):

$$\frac{dE}{dS} = -78500 \cdot \frac{\rho Z}{AE} \cdot \log \cdot (\frac{1.166E}{J} + 1)(keV / cm) \qquad (1.11)$$

where J is the "mean ionization potential" which represents the average rate of energy transfer due to all possible inelastic events. From Berger and Selzer's expression (1964):

$$J = (9.76Z + \frac{58.5}{Z^{0.19}}) \cdot 10^{-3}(keV) \qquad (1.12)$$

Then, the energy loss along the step from (x,y,z) to (x_n,y_n,z_n) is given by

$$\Delta E = step \cdot \frac{dE}{dS} \qquad (1.13)$$

Under known experimental conditions, such as incident beam energy, incident angle, physical constants of the specimen, etc., each electron trajectory can be traced step by step as it travels in the sample by the above relations. A flow chart for this model is illustrated in figure 2.

1-2. The Plural Scattering Monte Carlo Model

The basic assumptions of the plural scattering Monte Carlo model are the same as those for the single scattering model, but the implementation is markedly different. The total length of the electron trajectory within the sample is taken to be the Bethe range R_B by using Simpson's rule to numerically evaluate the integral:

$$R_B = \int_0^E \left(\frac{-1}{\frac{dE}{dS}}\right) dE \qquad (1.14)$$

where (dE/dS) is the stopping power given by equation (1.11). The Bethe range is then divided into fifty segments of equal length which is assumed to be the step of each scattering event. The energy of the electron at the start of the nth step is found by

$$E[n] = E[n-1] - \int_{step} \left(\frac{dE}{dS}\right) dS \qquad (1.15)$$

where (dE/dS) is again the stopping power, E[1] is set to be incident energy E0, and E[51] is set to be zero.

The azimuthal scattering angle is given by equation (1.7) again. The scattering angle

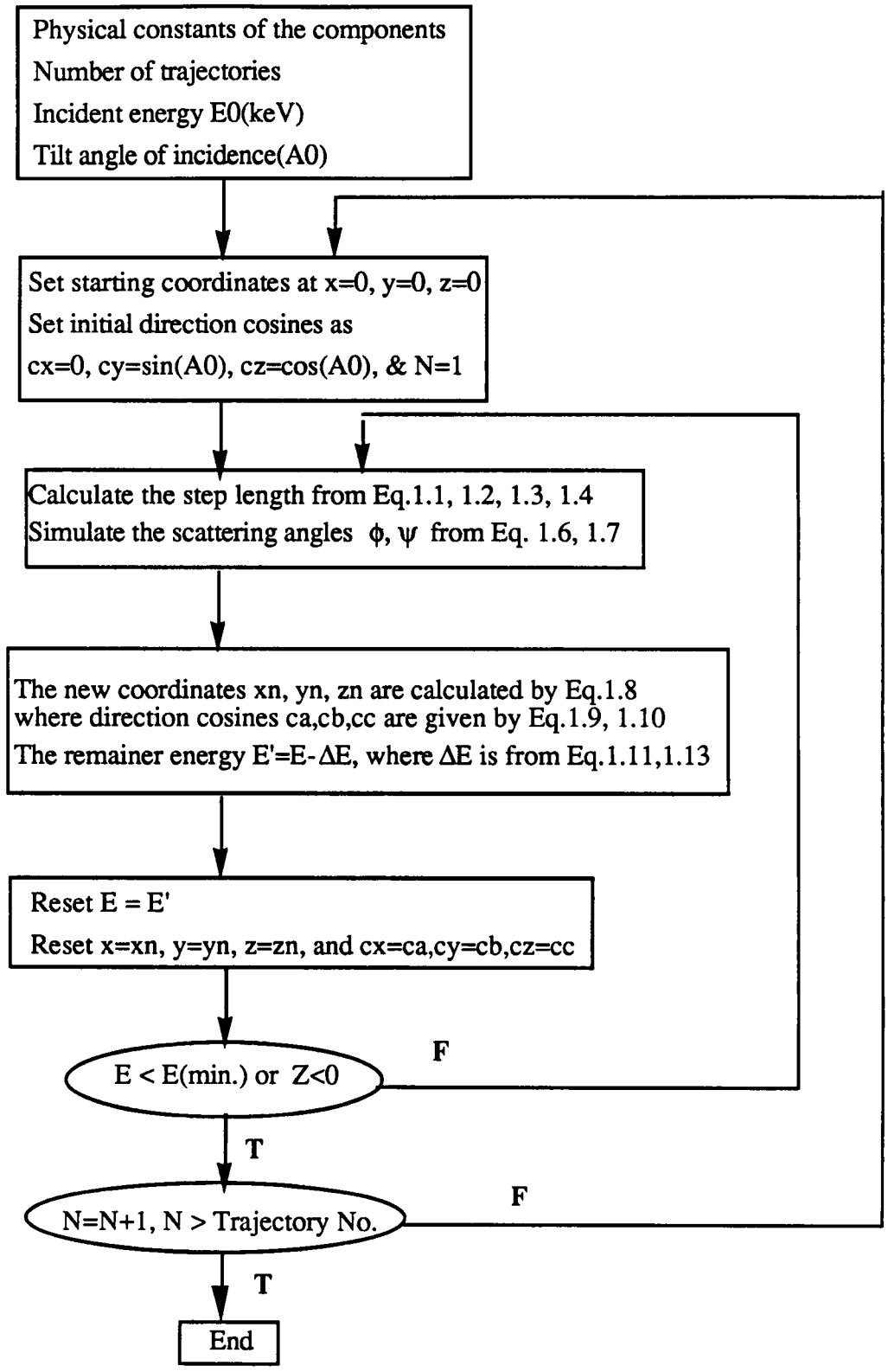

Figure 2. Flow chart for single scattering Monte Carlo model

ϕ is found by the initial idea of Curgenven and Duncumb(1971)

$$\tan(\frac{\phi}{2}) = \frac{b}{2p}(\frac{1}{\sqrt{RND}} - 1) \tag{1.16}$$

where b is $1.44 \times 10^{-2} Z/E$, E is the instantaneous energy of the electron in keV, and p is the impact parameter. Love et al. (1977) rewrote the equation as

$$\tan(\frac{\phi}{2}) = \tan(\frac{\phi_0}{2})(\frac{E_0}{E})(\frac{1}{\sqrt{RND}} - 1) \tag{1.17}$$

where

$$\tan(\frac{\phi_0}{2}) = \frac{0.0144Z}{2pE_0} \tag{1.18}$$

where ϕ_0 gives the minimum scattering angle for the incident energy E_0, and it could be obtained from the backscattered coefficient η :

$$\tan(\frac{\phi_0}{2}) = 0.016697 + 0.55108\eta - 0.96777\eta^2 + 1.8846\eta^3 \tag{1.19}$$

where the backscattered coefficient η is found by Hunger and Kuchler (1979) for a material of atomic Z at incident beam energy E_0 as

$$\eta(Z,E) = E_0^m C \tag{1.20}$$

where

$$m = 0.1382 - \frac{0.9211}{\sqrt{Z}} \tag{1.21}$$

and

$$C = 0.1904 - 0.2235(\ln Z) + 0.1292(\ln Z)^2 - 0.01491(\ln Z)^3 \tag{1.22}$$

The Monte Carlo loop then follows the procedure described above and the flow chart is shown in figure 3.

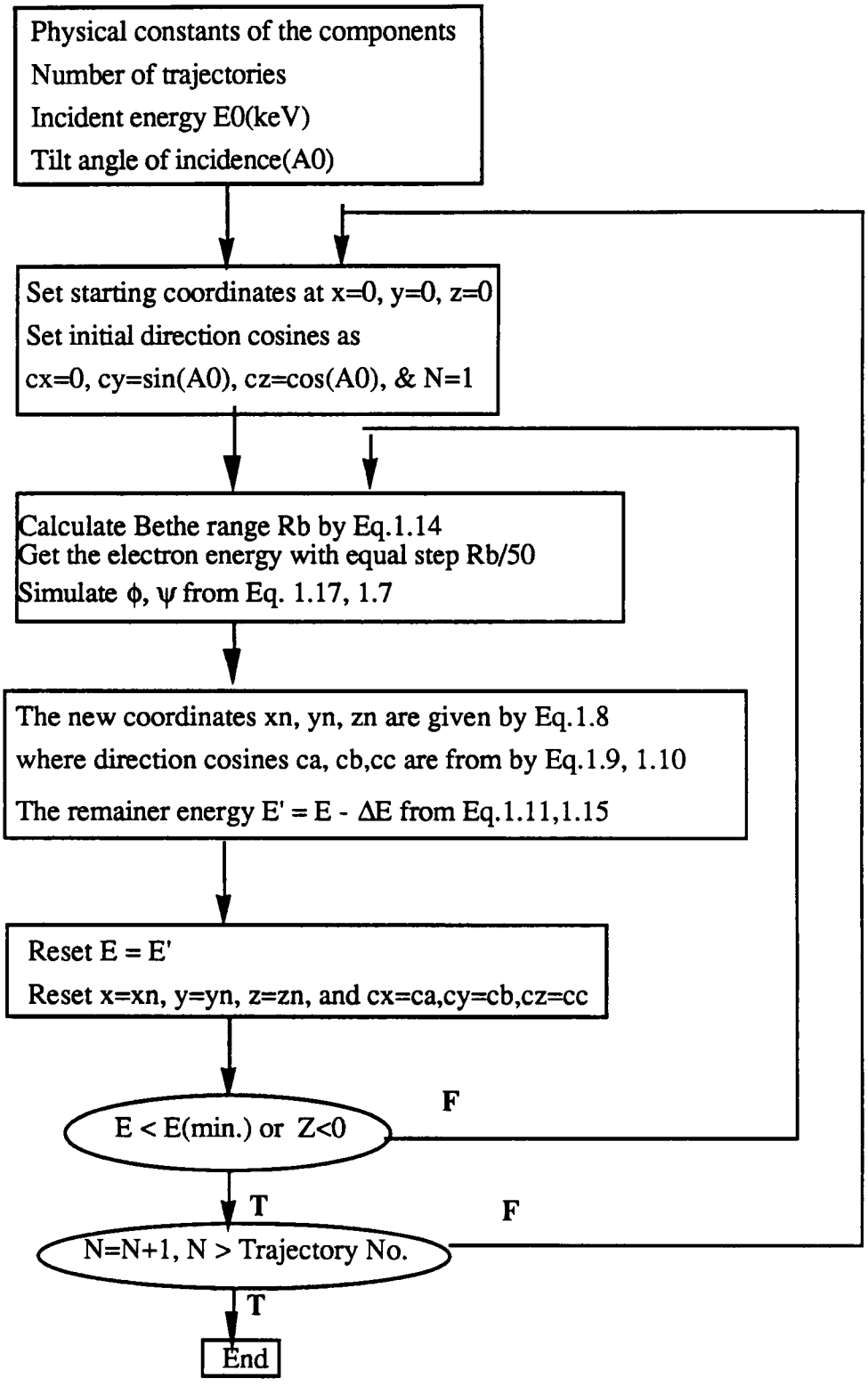

Figure 3. Flow chart for plural scattering Monte Carlo model

CHAPTER 2

DIFFUSION MATRIX MODEL

2-1. Introduction

Monte Carlo techniques have been used successfully to simulate electron-solid interactions and hence to compute the backscattered electron coefficient, secondary electron yield, the depth distribution of x-ray production, and the intensity of the continuum and characteristic x-ray radiation from a material of given composition and topography under specified experimental conditions. In principle therefore Monte Carlo modeling could be used as the basis of a quantitative method by matching experimental and computed data.

However, the practical problem is that this procedure is impracticably slow. To produce a simulation of acceptable statistical precision requires the computation of several thousand electron trajectories. Even on high speed parallel computers this requires several minutes while on less capable machines it may take from ten minutes to an hour, and any change of experimental parameters requires a fresh computation.

Hence, in this paper I describe a method which permits the BSE and SE signals and the intensity of the continuum and characteristic x-ray of a given structure to be computed within a fraction of a second without the need for a new set of Monte Carlo calculations. The procedure used is that of a diffusion matrix in which the strength of individual diffusion sources is found by an initial Monte Carlo computation.

2-2. The Development of the Diffusion Matrix Model for SE and BSE Signals

Calculation of Backscattered Electron Yield

The diffusion matrix method described here is developed from initial ideas of Desai and Reimer (1990), Czyzewski and Joy (1991), and Wang and Joy (1991). Basically, a Monte Carlo simulation is used to determine the magnitudes of an array of BS and SE sources embedded in a matrix which will reproduce the observed parameters of the interaction.

In the model, the specimen is set up so that the beam is traveling into the specimen along the positive z-axis. The y-axis lies along the surface in the direction of the intended surface profile, and the x-axis runs parallel to any surface geometrical structure. The interaction volume of the beam with the solid is divided into boxes of equal size Δz by Δx where Δz and Δx are each taken to be R/20, where R is the Bethe electron range in the material for electrons of the specified incident energy E_0.

The magnitude of the diffusion matrix element $BSE(z_i,x_j,\alpha_k)$ then contains the number of backscattered electrons that pass through the cell with coordinates z_i,x_j and BSE take-off angles α_k, where α_k is the angle measured from the positive z-axis to the exit direction of the backscattered electrons counterclockwise, which is illustrated in figure 4. As any electron crosses the cell in any scattering direction, it is accumulated as a contribution to the BSE signal, and the matrix which contains all possible exit angles at each cell is therefore obtained for the specimen of interest at specific impact energy E_0. For an arbitrary topography, the matrix is computed so that only those backscattered electrons which would leave the surface and strike a detector subtending a specified solid

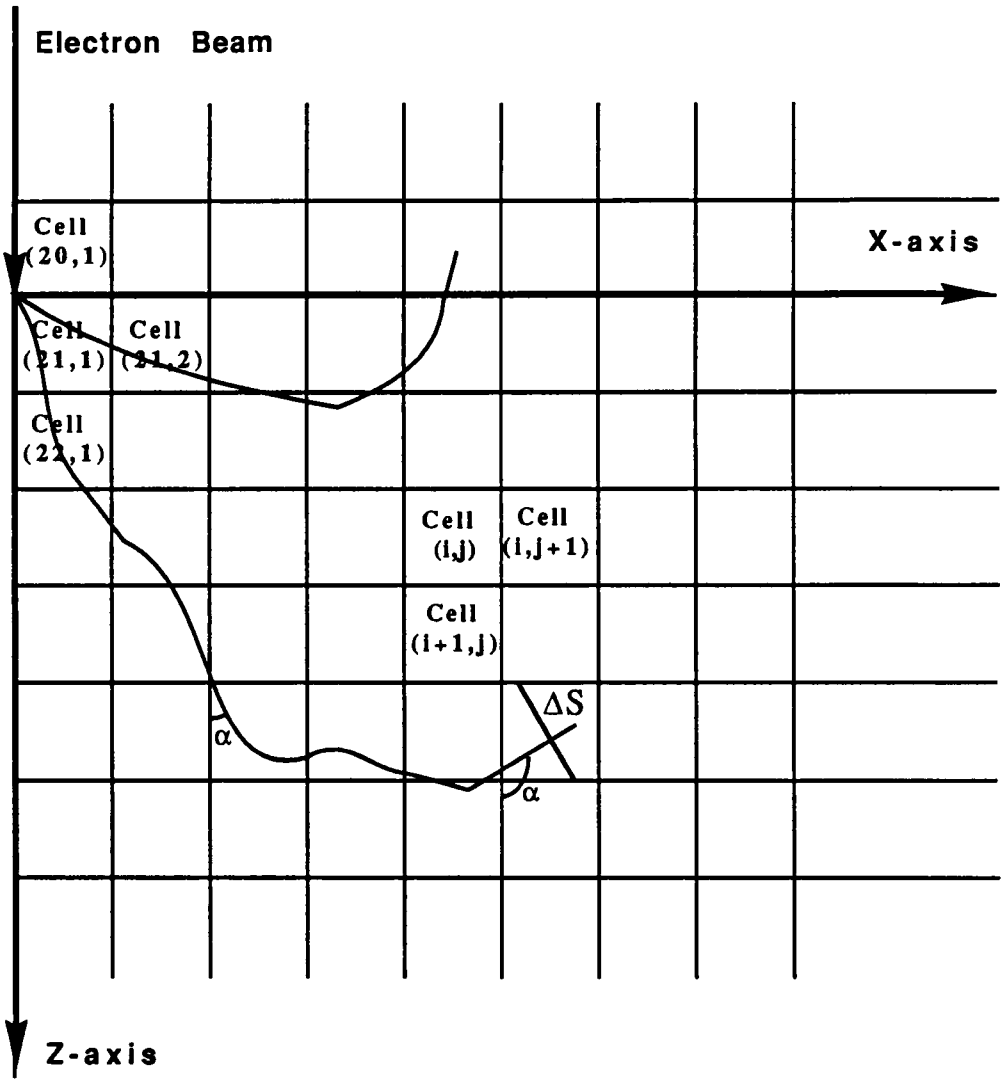

Figure 4. The schematic geometry of the diffusion matrix. The magnitude of the matrix element gives the numbers of BSE, SE passing through cells at the take off angle α.

angle Ω at the specimen are included. Several different detector geometries can be simultaneously computed from the same Monte Carlo runs so that the effects on the profile of changing the detector position can also be evaluated without the need for further simulations. The results are stored in a 40 x 20 x 36 matrix for $-R < z < R$ and $0 < x < R$ in steps of R/20, and $0° < \alpha_k < 360°$ in steps of 10° for all the take off angles in space. Note that only the positive y direction is considered in the matrix model because of the symmetry of the electron trajectory as the electron travels in the specimen.

Calculation of Secondary Electron Yield

The secondary electrons are assumed to be generated solely by the exiting backscattered electrons. The secondary yield δ is then given by the expression of Drescher et al. (1970),

$$\delta = \left(\frac{E}{E_{BSE}}\right)^{-0.8} \sec \xi \qquad (2.1)$$

where E is the incident energy, E_{BSE} is the energy of the emerging backscattered electron, and ξ is the angle between the backscattered electron and the surface normal as it leaves. Likewise, the diffusion matrix $SE(z_i,x_j,\alpha_k)$ contains the secondary electrons crossing the cell, excluding the item $\sec\xi$, is created simultaneously as BSE matrix, where z_i,x_j is the coordinate of the cell, and α_k is again the take off angle of the backscattered electrons, which will be used to compute ξ on a specified profile.

2-3. The Extension of the Diffusion Matrix Model to X-ray Generations

Calculation of Bremsstrahlung X-ray Intensity

The speed of the diffusion matrix method makes it attractive for other application. Here we discuss the extension of the method to the computation of x-ray spectrum. The theoretical model for the calculation of the cross-section, and intensity of the bremsstrahlung and characteristic x-rays is described as follows (Fiori 1982, Joy 1986):

As a beam electron passes through the Coulomb field of an atom, it can undergo deceleration and decrease the magnitude of its velocity and its kinetic energy. The lost kinetic energy is emitted as a photon of electromagnetic radiation by the beam electron. The generation of radiation along an electron path is usually discussed in terms of the "ionization cross-section", $Q(cm^2)$, which is the probability that a process will occur. Several cross-sections for the production of bremsstrahlung by energetic electrons are available in the literature. Sommerfeld (1931,1950) developed a theory of continuum generation that neglects the presence of atomic electrons (screening) and assumes a pure Coulomb field about a point nucleus. Relativity, electron spin, and retardation of potential are neglected, and the incoming electron and scattered electron are represented by plane waves that occupy all space. The Sommerfeld theory is troublesome to evaluate because of its mathematical form. Numerical estimates for selected atomic numbers and values of photon and electron energies have been made by Kirkpatrick and Wiedmann (1945).

If the radiation is assumed to be isotropic, an average cross-section is given by

$$Q = 4\pi \cdot \frac{2}{3} \cdot \frac{(I_x + 2I_y)}{E_b} \tag{2.2}$$

where

$$I_x = \frac{0.2998Z^2}{E}\left|0.252 + a[(\frac{E_b}{E}) - 0.135] - b[(\frac{E_b}{E}) - 0.135]^2\right| \times 1.51 \times 10^{-24} \tag{2.3}$$

where

$$a = 1.47B - 0.507A - 0.833 \tag{2.3a}$$

$$b = 1.70B - 1.09A - 0.62 \tag{2.3b}$$

$$A = \exp(-\frac{0.223E}{0.2988Z^2}) - \exp(-\frac{57E}{0.2988Z^2}) \tag{2.3c}$$

$$B = \exp(-\frac{0.0828E}{0.2988Z^2}) - \exp(-\frac{84.9E}{0.2988Z^2}) \tag{2.3d}$$

and

$$I_y = I_z = \frac{0.2988Z^2}{E}\left|-j + \frac{k}{(Eb/E) + h}\right| \times 1.51 \times 10^{-24} \tag{2.4}$$

$$h = \frac{-0.214 \cdot y1 + 1.21 \cdot y2 - y3}{1.43 \cdot y1 - 2.43 \cdot y2 + y3} \tag{2.4a}$$

$$j = (1 + 2h) \cdot y2 - 2 \cdot (1 + h) \cdot y3 \tag{2.4b}$$

$$k = (1+h)\cdot(y3+j) \tag{2.4c}$$

$$y1 = 0.22\cdot[1.0 - 0.39\cdot\exp(-\frac{26.9E}{0.2988Z^2})] \tag{2.4d}$$

$$y2 = 0.067 + \frac{0.023}{[(E/_{0.2988Z^2}) + 0.75]} \tag{2.4e}$$

$$y3 = -0.00259 + \frac{0.00776}{[(E/_{0.2988Z^2}) + 0.116]} \tag{2.4f}$$

Due to the intrinsic dependence on the direction of the incident beam, some anisotropy is expected although the randomness of the electron scattering could reduce the degree of anisotropy. So the radiation intensity in the direction of the detector has to be calculated from the geometry of the electron trajectory.

The cross-section considering the relativistic effects correction was given by Motz and Placious (1958)

$$Q_{K-W} = [\frac{I_x(1-\cos^2\theta) + I_y(1+\cos^2\theta)}{(1-\beta\cos\theta)^2}] / E_b \tag{2.5}$$

where

β is the relativistic correction factor and given by

$$\beta = \frac{\upsilon}{c} = \sqrt{1-[1+(E/_{511})]^{-2}} \tag{2.6}$$

θ is the angle between the observation direction and the electron direction and can be calculated from two vectors, which is shown in figure 5

$$\vec{A} = step \cdot \cos(\phi_x)\vec{x} + step \cdot \cos(\phi_y)\vec{y} + step \cdot \cos(\phi_z)\vec{z} \qquad (2.7a)$$

$$\vec{B} = -step \cdot \cos(t.o.a.)\vec{x} - step \cdot \sin(t.o.a.)\vec{z} \qquad (2.7b)$$

$$\cos\theta = \frac{\vec{A}\cdot\vec{B}}{|\vec{A}|\cdot|\vec{B}|} = -\cos(\phi_x)\cdot\cos(t.o.a.) - \cos(\phi_z)\cdot\sin(t.o.a.) \qquad (2.7c)$$

where t.o.a. = take-off angle

New expressions were employed by Statham (1976) to improve the fit for $E/Z^2 <$ 0.0604 where Kirkpatrick and Wiedmann's expression seems to fit data badly. The reversed expressions are

$$X = [-1.01904 + 0.146014\cdot(\frac{E_b}{E}) - 0.0501077\cdot(\frac{E_b}{E})^2] \times \log_e(\frac{E}{0.2988Z^2}) \\ -1.48311 + 0.947484\cdot(\frac{E_b}{E}) - 0.350014\cdot(\frac{E_b}{E})^2 \qquad (2.8a)$$

$$Y = [-0.882129 + 0.366934\cdot(\frac{E_b}{E}) - 0.339646\cdot(\frac{E_b}{E})^2] \times \log_e(\frac{E}{0.2988Z^2}) \\ -1.04088 - 1.86355\cdot(\frac{E_b}{E}) - 0.723068\cdot(\frac{E_b}{E})^2 \qquad (2.8b)$$

$$I_x' = \exp(X), \text{ and } I_y' = \exp(Y) \qquad (2.9)$$

where E is the incident energy, and E_b is the bremsstrahlung photon energy.

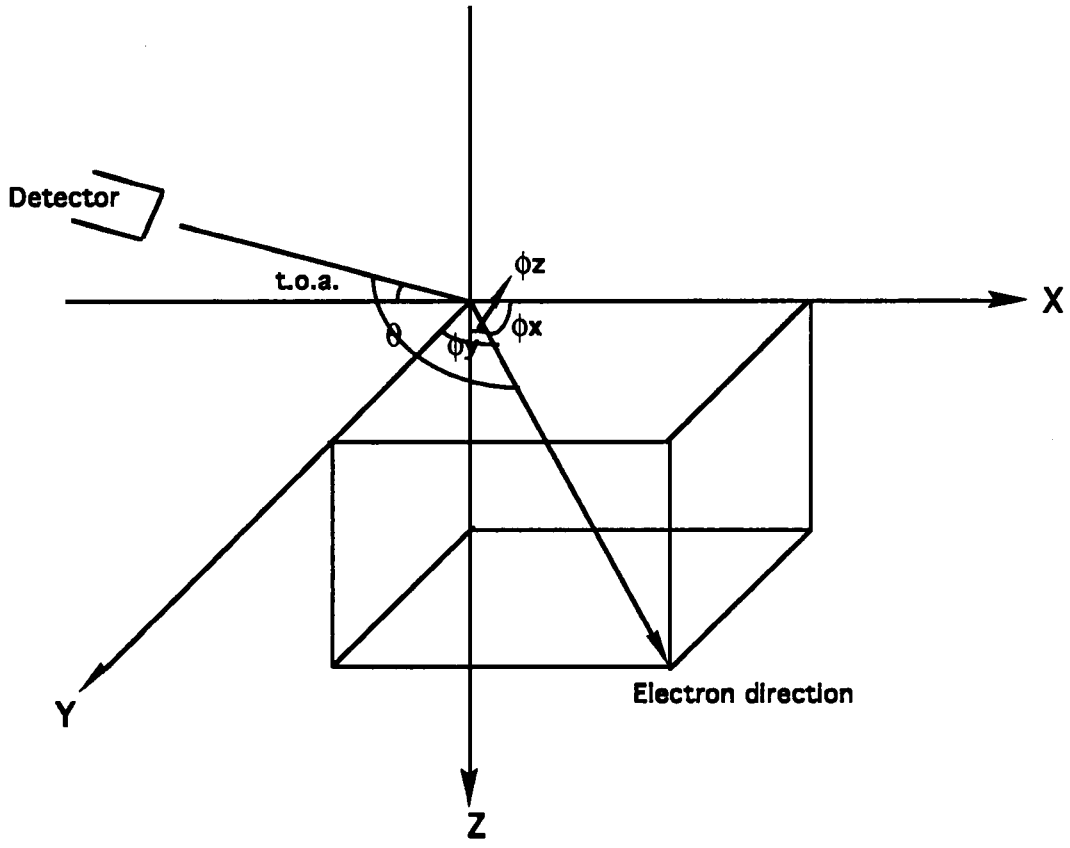

Figure 5. Schematic diagram of geometrical relationships between the observation direction and electron direction for any single trajectory. Here t.o.a. is take off angle.

In the above equations, note that transformations have been applied from electrostatic units to keV and in units of I from erg/sr/unit frequency interval/(atom/cm^2) to keV/keV energy interval/sr/(atom/cm^2). They are conveniently changed to units of keV per keV energy interval on multiplication by 1.509 x 10^{-24}.

The number of bremsstrahlung x-ray photons I_{Brem} produced by a single incident electron is then found from the relation:

$$I_{Brem} = \frac{N}{A} \int_{path} Q d(\rho x) \qquad (2.10)$$

where N is Avogadro's number, A is the atomic weight of the specimen, ρ is the density in gm cm^{-3}, x is the distance along the electron path in cm, and the matrix $BR(z_i,x_j,E_b)$ that contains the numbers of bremsstrahlung x-ray generation I_{Brem} is developed from the same Monte Carlo run, where z_i,x_j represents the coordinates of the grids, E_b is the photon energy of bremsstrahlung x-rays, -R<z<R and 0<x<R in steps of R/20, and 1< E_b < E_0 in steps of E_0/30. For each incident beam energy and material of interest, all the generated bremsstrahlung x-ray intensity is accounted and stored in the relevant cells during the impaction of the electron and the atom. The diffusion matrix with 40x20x30 array is then ready for bremsstrahlung EDS spectrum computation at any given structure of the topography. Note that the detector geometry is fixed in the program because of the limitation of RAM of the computer, i.e., a fourth dimension is expected to record the changeable detector geometry for more flexible usage of the program.

Calculation of Characteristic X-ray Intensity

The beam electrons can also interact with a tightly bound inner-shell electron and eject it from the atom. The number of characteristic x-rays generated into 4π steradian is expressed as

$$I_{ch} = \frac{\sigma_k \omega N_0}{A} \cdot \rho \Delta z \qquad (2.11)$$

where σ_k is the ionization cross section for the shell of interest and has dimensions of area; N is Avogadro's number; A is the atom weight; ρ is the density of the specimen; Δz is the thickness that the electron travels; ω, the fluorescent yield, is the probability that an x-ray will be emitted due to the ionization of a given shell and calculated from a semi-empirical expression due to Burhop (1955)

$$(\frac{\omega}{1-\omega})^{\frac{1}{4}} = A + BZ + CZ^3 \qquad (2.12)$$

where the constants A, B, C for L, M shell are given by Colby (1968).

An empirical approach to K-shell ionization cross-section by electrons is illustrated here. By using Casnati's empirical expression (1982), σ_k is found by

$$\sigma_k = n_k a_0^2 R(\frac{I_0}{I_k})^2 \psi\varphi \frac{\ln U}{U} \qquad (2.13)$$

where $n_k = 2$ for k shell

$a_0 = 5.292e^{-11}$ m, the first Bohr radius.

I_0 = 0.013606 keV, the Ryberg energy.

I_k is the edge energy (E_c)

with

$$\psi = \left(\frac{I_k}{I_0}\right)^{(d_0 + d_1/U + d_2/U^2)} \tag{2.14}$$

where d_0 = -0.0318, d_1 = -1.736, d_2 = -0.1135

$$\varphi = b_0 \cdot \exp\left(\frac{b_1}{U} + \frac{b_2}{U^2}\right) \tag{2.15}$$

where b_0 = 10.57, b_1 = -1.736, b_2 = 0.317

where R is the effect of the relativistic correction for these subshell and given by

$$R = \frac{(1 + E_0/mc^2)^2}{(1 + E_0/2mc^2)} \tag{2.16}$$

where E_0 is the impact energy of incident electron, m is the rest mass of the electron, and c is the velocity of light in vacuum.

For l, m shell, the empirical model developed by Schreiber et al., (1981) is used here to evaluate the value of the ionization cross-section. The ionization cross-section $Q_{x,l}$ for shell l of element x is written as

$$Q_{x,l} = \pi e^4 n_s \frac{b \log(cU_x)}{E_x^2 U_x^d} \tag{2.17}$$

where, $\pi e^4 = 6.4924 \times 10^{-20}$, n_s is the number of electrons in the shell l, E_x is the absorption edge energy (keV) for shell l of element x, $b_L = 0.2704 + 0.00726\ (\log Z)^3$, $b_M = 11.33\text{-}2.43\ (\log Z)$, $c_L = c_M = 1$, $d_L = d_M = 1$. $U_x = E_0/E_x$ is the overvoltage, where E_0 is the beam voltage (keV).

Likewise, the diffusion matrix $CH(z_i,x_j,n_s)$ then contains the characteristic x-rays photons that pass through the cell centered at z_i,x_j, during the Monte Carlo simulation, where n_s represents any shell of the element in the range from 1 to 3, which refers to K, L, M shell respectively.

The accuracy of the matrix depends on the quality of the Monte Carlo simulation used to generate it. For the work described here, I have used a standard plural scattering model but with a parametrically modified screened Rutherford scattering cross-section, which is described in detail in chapter one. In order to provide adequate statistics for each cell of the matrix, 50,000 trajectories were used for each beam energy and material of interest.

2-4. Calculation of a Signal Profile

To calculate the BSE and SE profiles from an arbitrary surface geometry we proceed on a point-by-point basis. For each beam incidence position we lay down a grid identical to that used for the original matrix computation, placing the origin at the beam point . The positive Z axis is parallel to the beam direction, the positive X axis is to the right, and the positive Y axis is out of the plane of the drawing. The topography profile is

then divided into segments defined by the interaction of the surface and grids. Each segment is specified by two coordinates I and J, which give its Z and X positions relative to the impact point (figure 6), and its tilt angle α to the Z-axis. We assume that any electron whose take-off angle is greater than the tilt angle can escape from the surface and have a contribution to the backscattered electron coefficient, and also to the secondary electron yield. Yet the factor $\sec\xi$ should be multiplied to each cell of the SE matrix on a specified profile calculation, where ξ is the angle between the backscattered electron and the surface normal. If α is not equal to one of the stored angles then the desired value is found by linear interpolation between the adjacent stored angular values. The signal contributions from each segment must also be normalized because the width of the strip Δs for which the matrix was calculated is in general different from the actual width. The BSE and SE signals for this particular beam impact position are then found by summing the contributions from all of the segments, i.e., segments, S1,S2,S3 etc., to the right and T1,T2,T3,etc., to the left of the impact point. This process is then repeated for every other beam position until the complete profile is generated. Note that since the emission is computed for an array of strips in the x direction, the surface which is being modeled need not be planar, but can be of arbitrary shape -- e.g., edges could be rounded rather than sharp, and surface could be either concave or convex rather than flat.

The bremsstrahlung x-ray energy dispersive spectrum for a particular beam impact position is found by summing the contributions from all of the cells in the bulk specimen, i.e., cells S(1,1), S(1,2), S(1,3)... and S(2,1), S(2,2), S(2,3)... etc. to the right and T(1,1), T(1,2), T(1,3)... etc. to the left of the impact point (figure 7). Two additional factors should be considered in the calculation of emitted x-ray signals:

1). As x-rays of a given energy E and incident intensity I_0 pass through a slab of

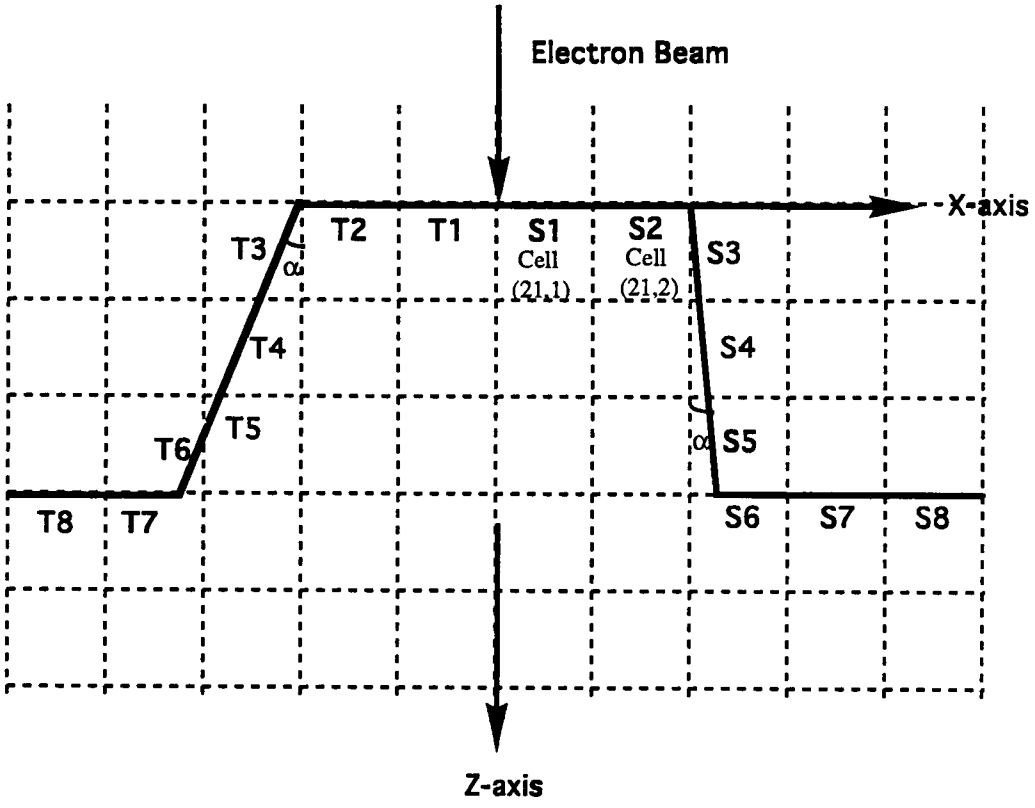

Figure 6. Schematic illustration of method to calculate a BSE, SE signal profile for a given geometry structure from the diffusion matrix. The grid is set up with the incident beam point as origin and contributions are summed from each of the surface segments.

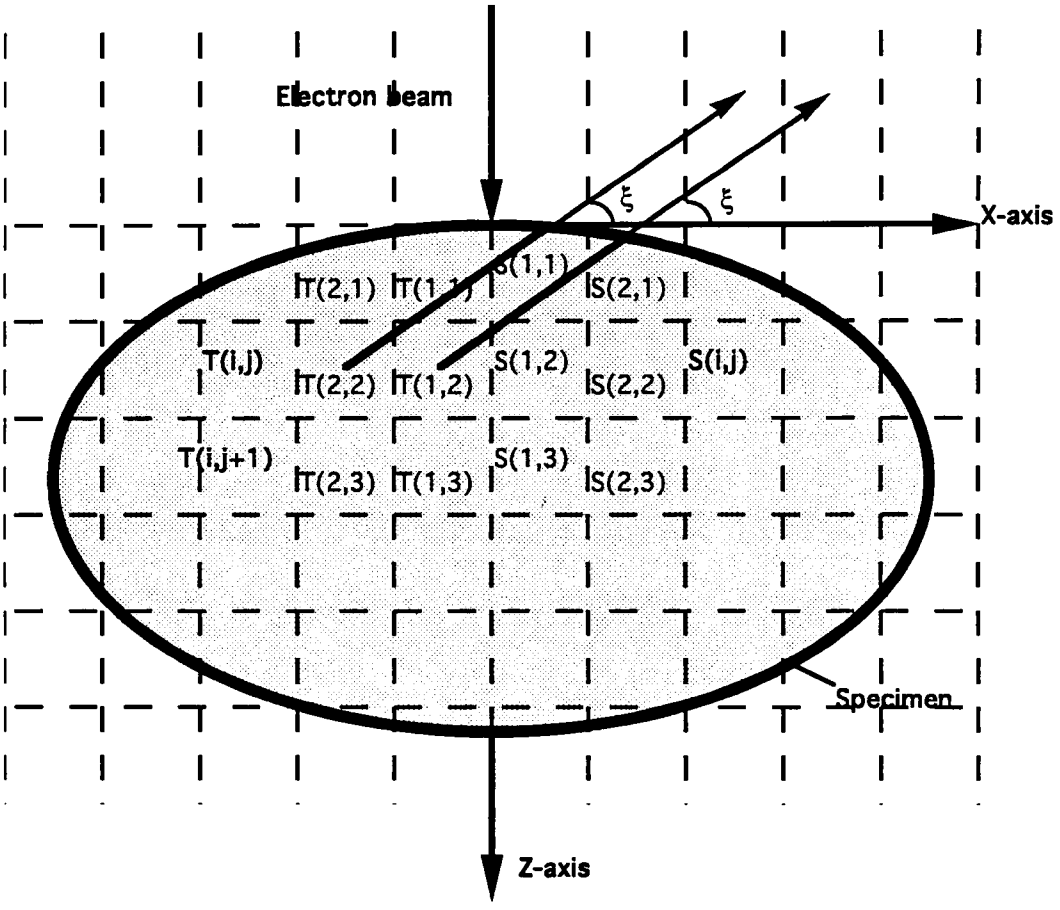

Figure 7: Schematic illustration of diffusion matrix model applied to a round topography sample for the simulation of bremsstrahlung x-ray intensity. All the grids inside the beam range are considered. Note that dark part on the exit direction refers to the actual path length.

thickness Z and density ρ, the intensity emitted, I, is attenuated according to the equation

$$\frac{I}{I_0} = \exp[-(\frac{\mu}{\rho})\rho Z] \qquad (2.18)$$

where (μ/ρ) is the mass absorption coefficient of the sample for x-rays.

Collections of mass absorption coefficients have been obtained by measurement, and fitted to convenient equations for calculation. Heinrich's model (1966) is most often used in this field, and is shown below μ(Z,E), where Z is the absorbing element and E the photon energy, is

$$A \cdot \exp[B \cdot \log^2(Z) + C \cdot \log(Z) + D] \times (\frac{12.398}{E})^F \qquad (2.19)$$

where A,B,C,D and F are constants and supplied by Russ (1984), e.g. for K shell

A = 1.00, B = -0.2322294, C = 4.070053, D = -6.220746,

F = exp (-0.0045522 $\log^2$(Z) - 0.00685351 log(Z) + 1.070181)

2). In order to compare the theoretical and the experimental results, the detector efficiency should be considered in the calculation of the emitted x-ray intensity due to the variance design of the detector.

The EDS spectrum for characteristic x-ray energy is simulated in a similar way to the bremsstrahlung x-ray energy dispersive spectrum.

For an arbitrary geometry sample, it is instructive to use cubic spline interpolation (Burden, 1989) between each successive pair of nodes to obtain all the coordinates required by the calculation. A coordinate system with its original point at the beam impact position is set up, then the coordinates of every pair of nodes where the curve doesn't have a continuous derivative are attained, so that we can determine all the coordinate of grids in the beam interaction volume by using cubic polynomial approximation at every subinterval. Generally, this process could be repeated for every other beam position where the EDS spectrum is expected.

To experimental test the matrix approach described above, some measurements have been performed for a series of flat pure elemental samples on SEM-800, Hitachi. The comparisons of the EDS from calculation by the diffusion matrix method and experimental results are shown in figure 8 for carbon, silicon, titanium at incident energy at 20keV, copper with incident energy at 20keV and 15keV, molybdenum, silver, tantalum, and platinum at incident energy at 25keV. The degree of agreement between the calculated and experimental results for Mo and Ag sample is not as good as for the other elements. This is because these particular samples were physically larger than the others, which changed the take-off angle for the detector. However, because of the difficulty in determining the true geometry, the same nominal parameters were used.

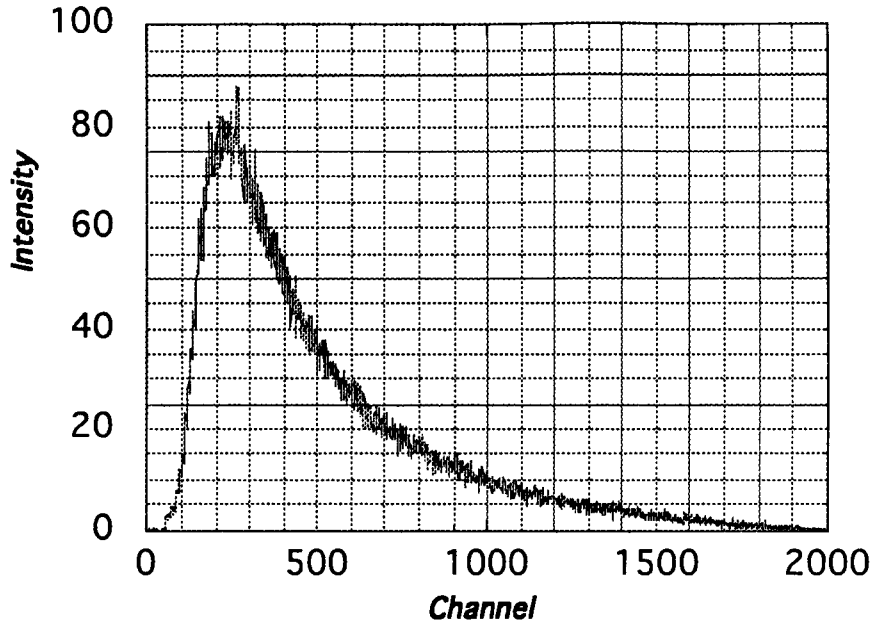

(I)

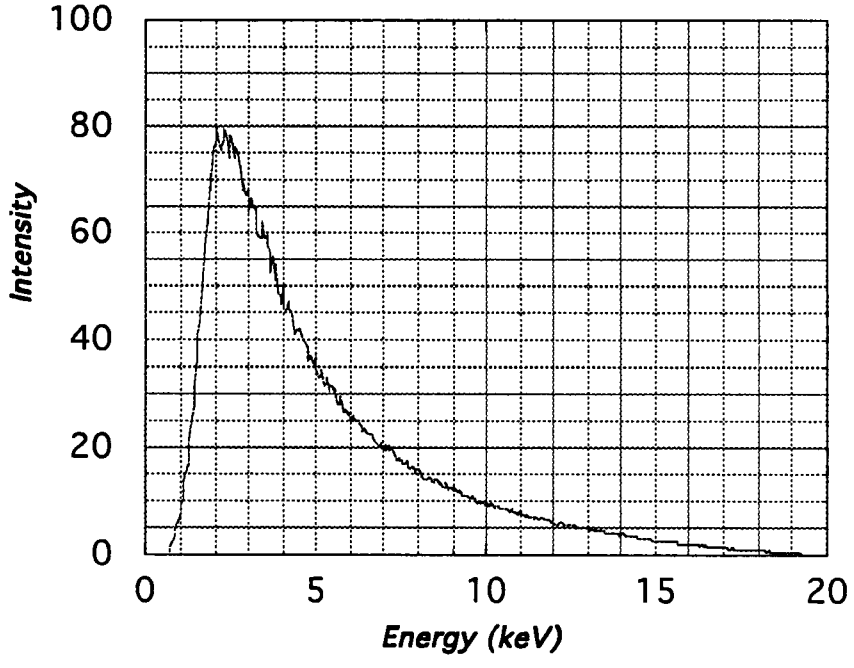

(II)

Figure 8. Comparison of EDS spectrum (I) measured at SEM-800, (II) calculated by diffusion matrix method. (a). Carbon at E0=20keV

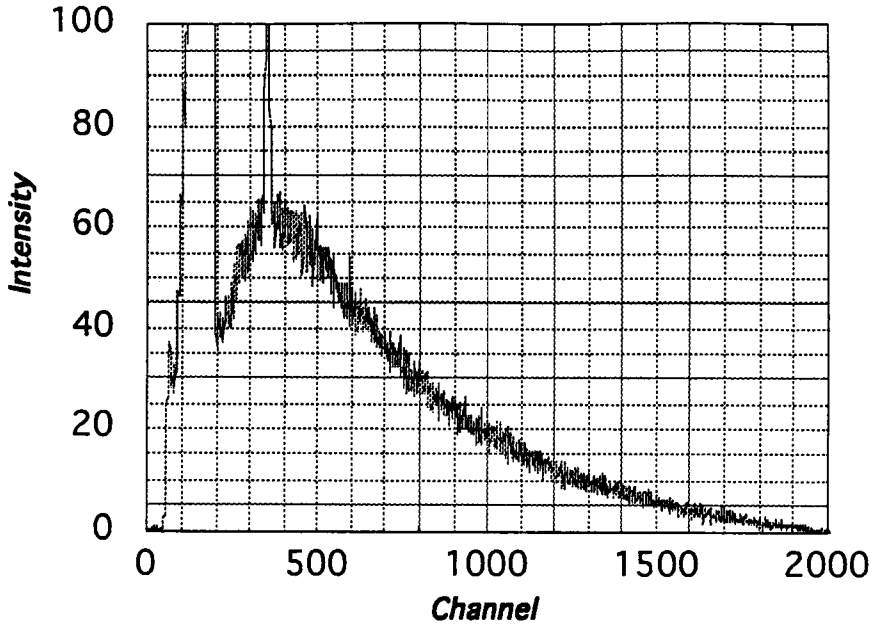

(I)

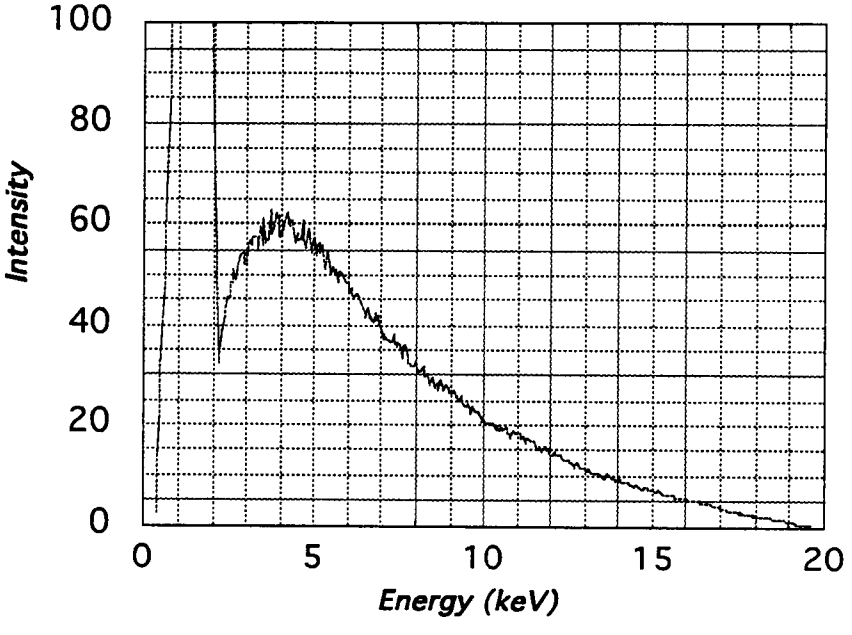

(II)

Figure 8. (continued) (b). Silicon at E0=20keV

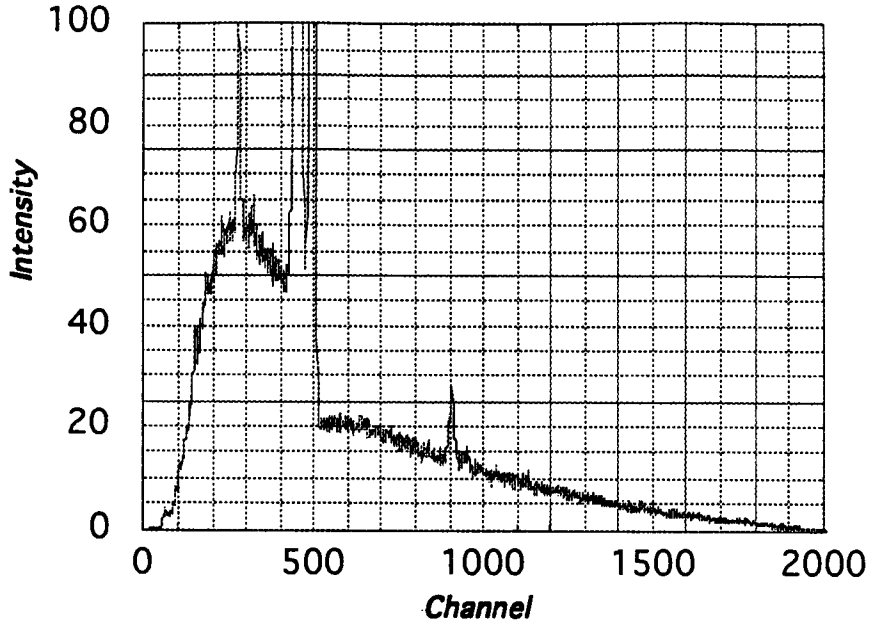

(I)

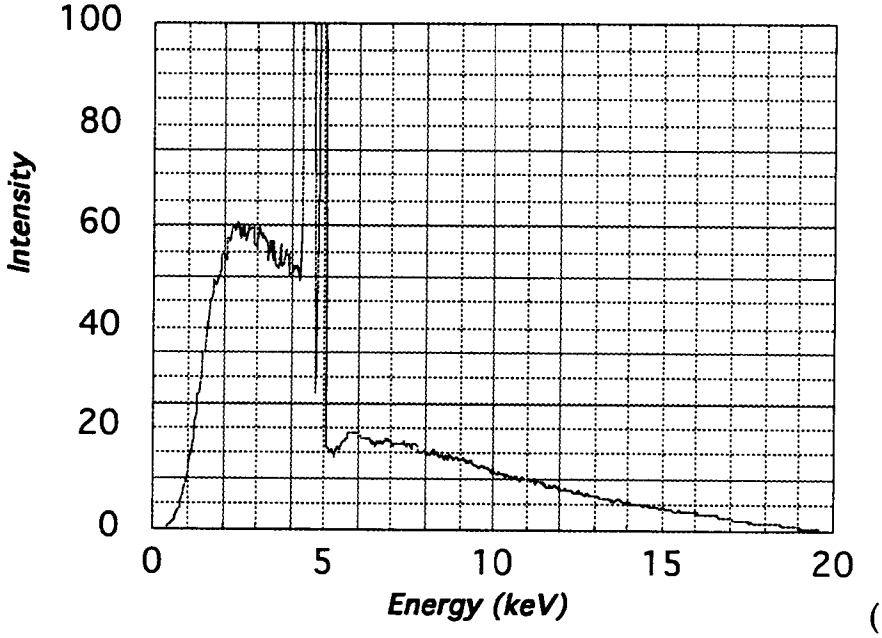

(II)

Figure 8. (continued) (c). Titanium at E0=20keV

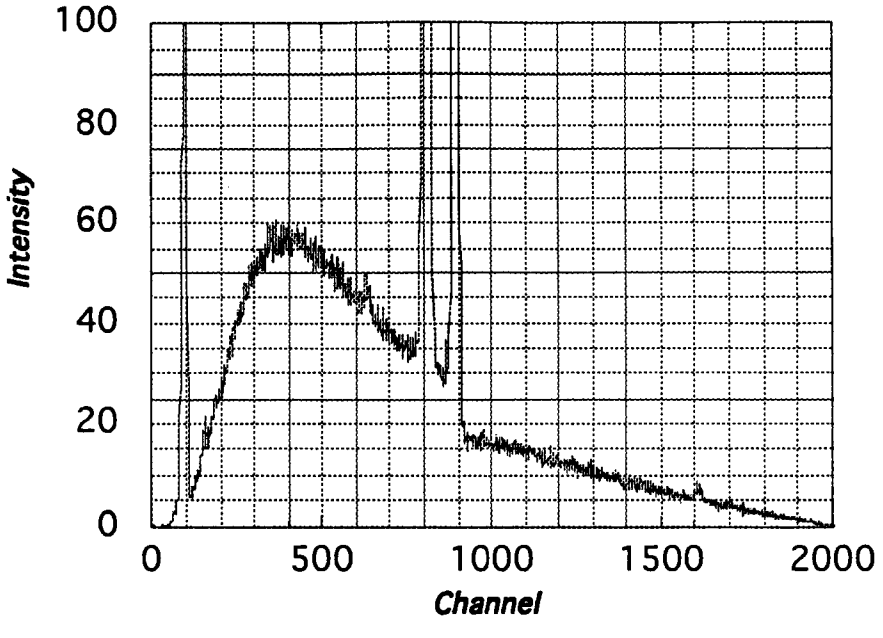

(I)

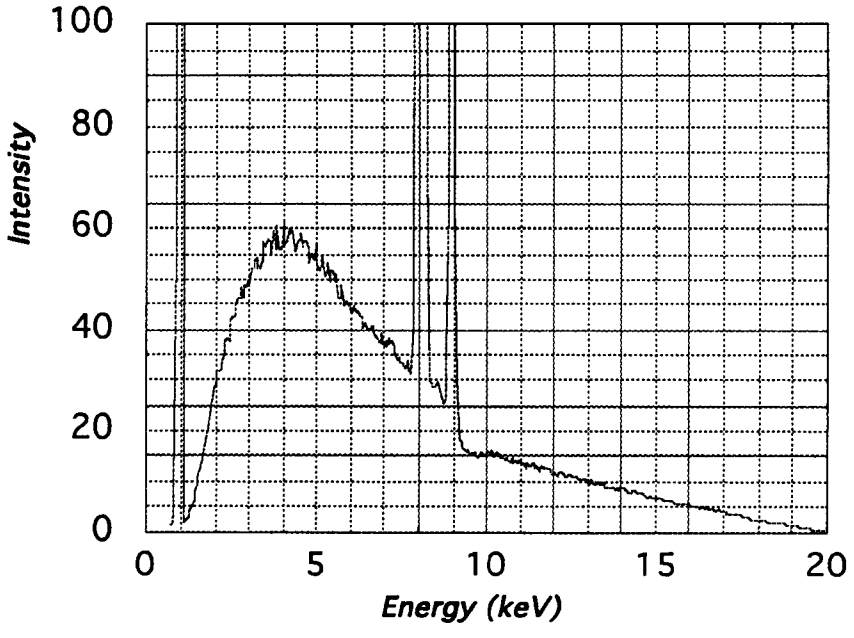

(II)

Figure 8. (continued) (d). Copper at E0=20keV

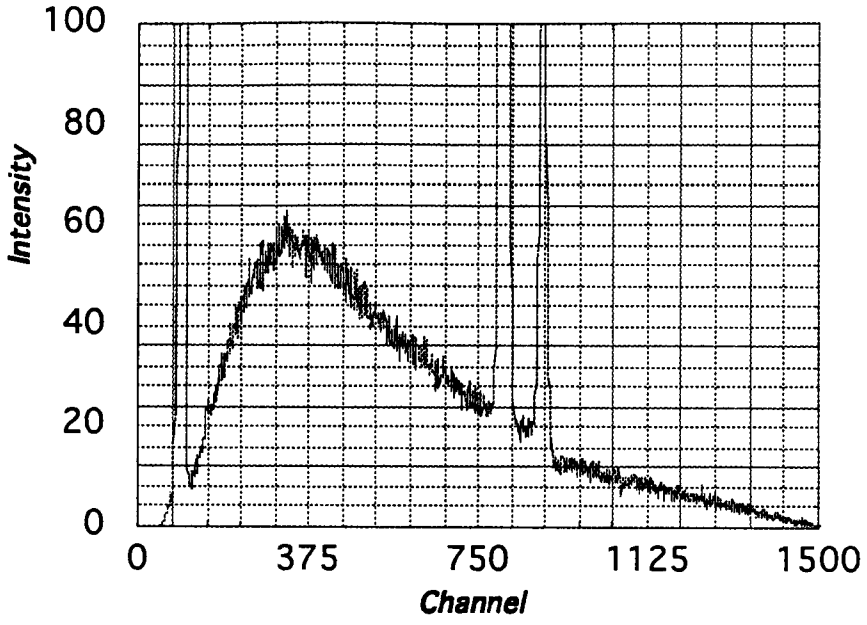

(I)

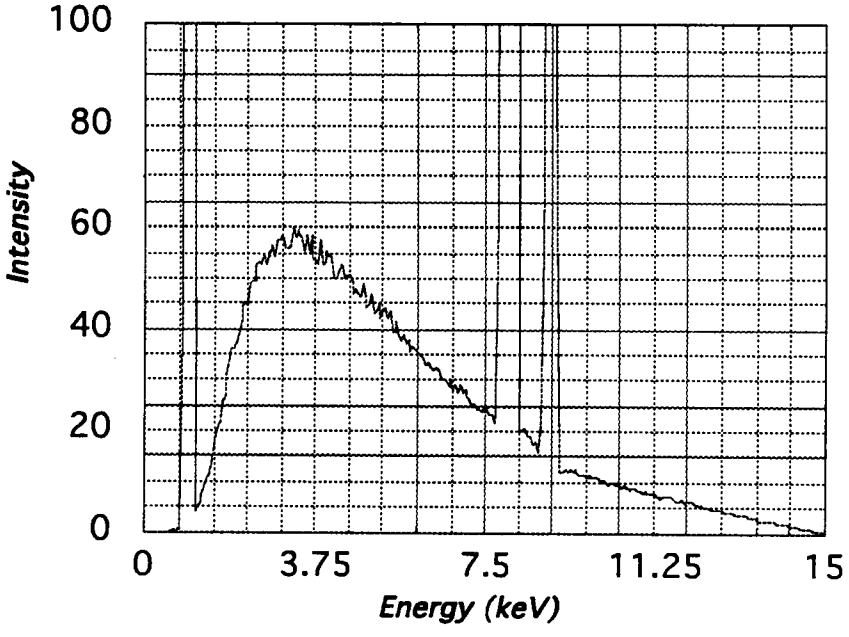

(II)

Figure 8. (continued) (e). Copper at E0=15keV

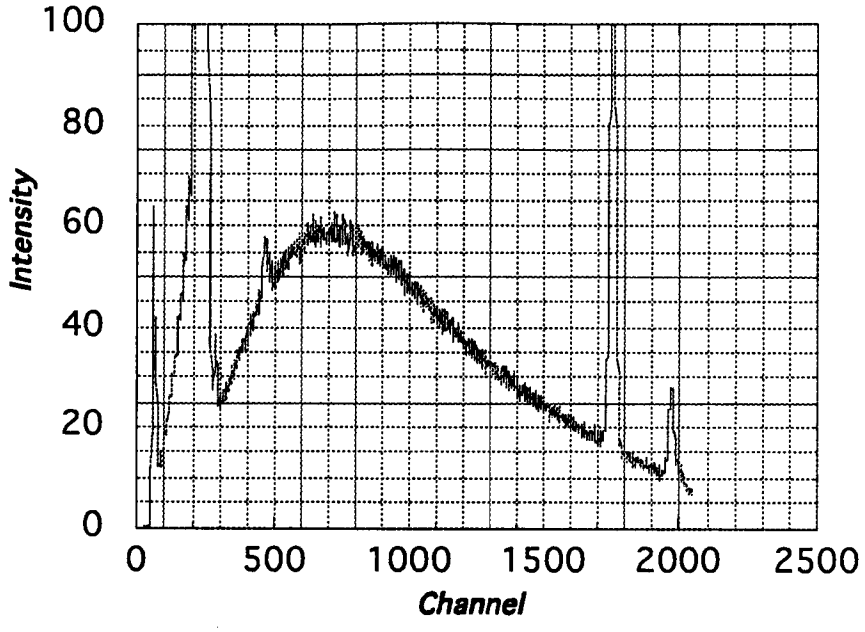

(I)

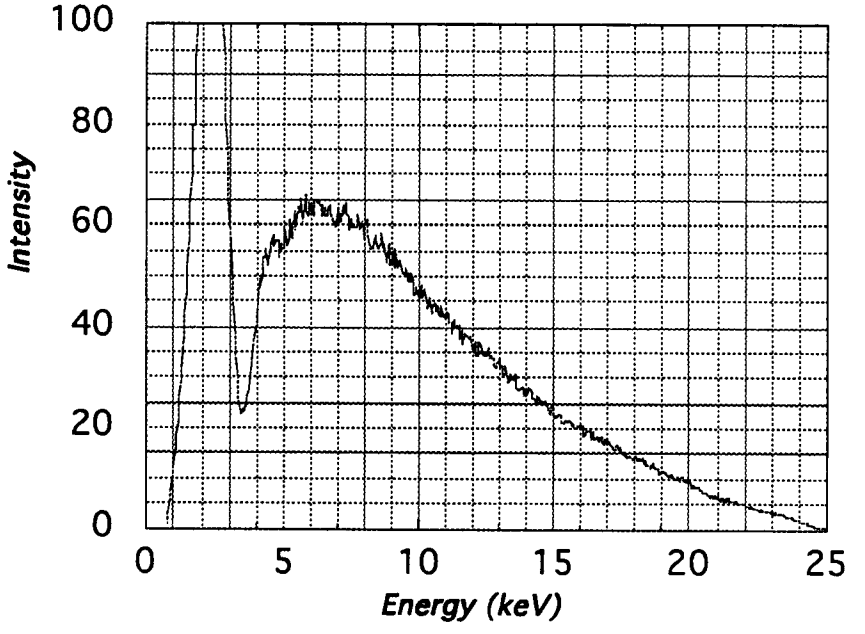

(II)

Figure 8. (continued) (f). Molybdenum at E0=25keV

Note that only bremsstrahlung x-ray spectrum is shown in (II)

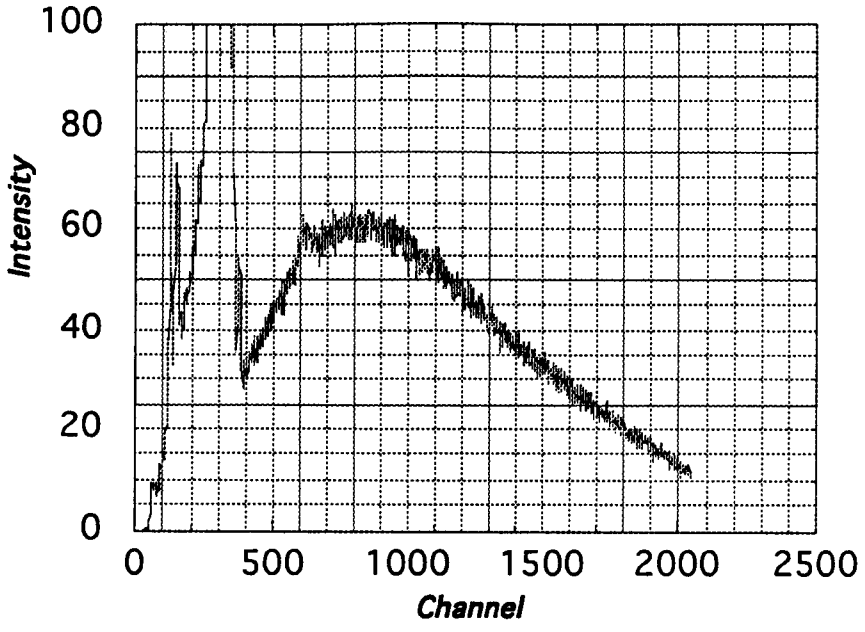

(I)

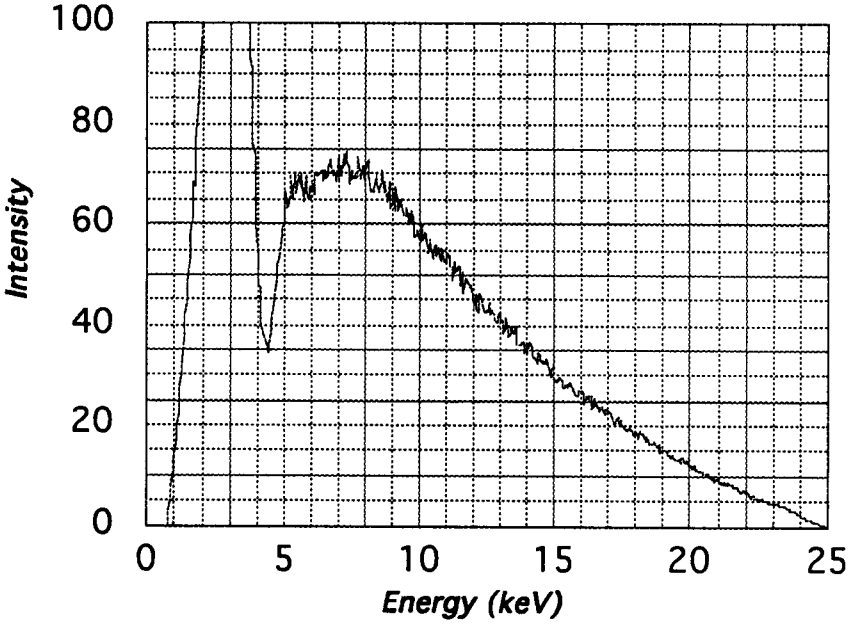

(II)

Figure 8. (continued) (g). Silver at E0=25keV

Note that only bremsstrahlung x-ray spectrum is shown in (II)

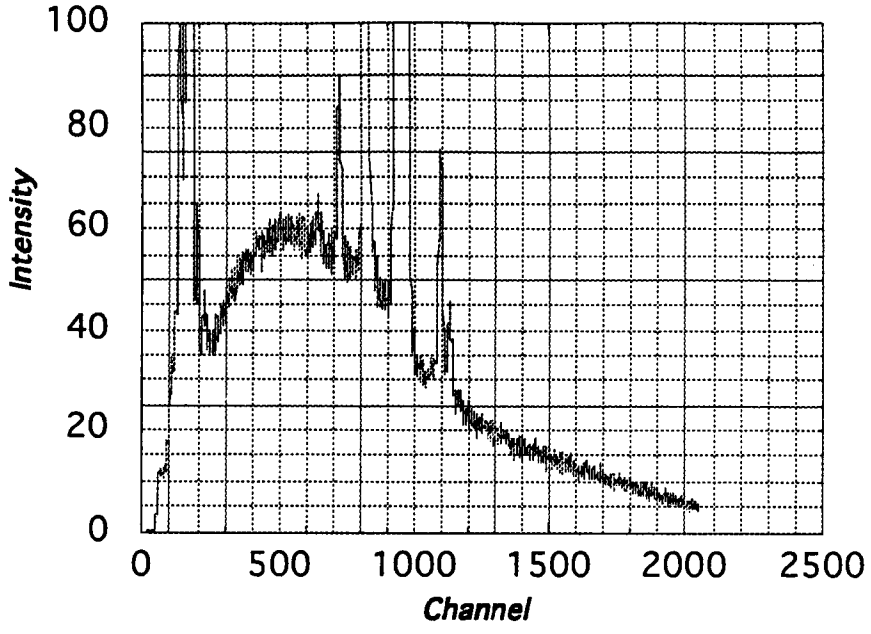

(I)

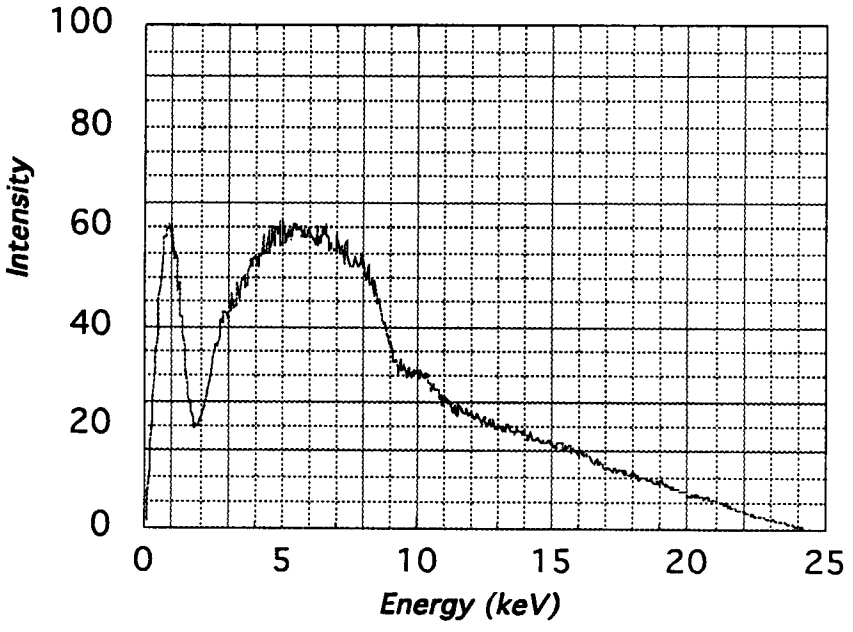

(II)

Figure 8. (continued) (h). Tantalum at E0=25keV

Note that only bremsstrahlung x-ray spectrum is shown in (II)

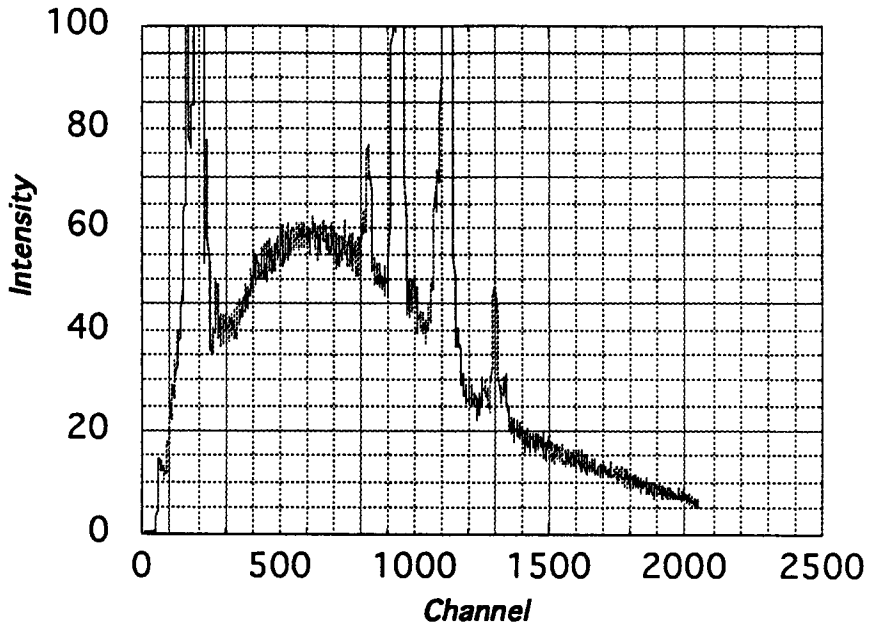

(I)

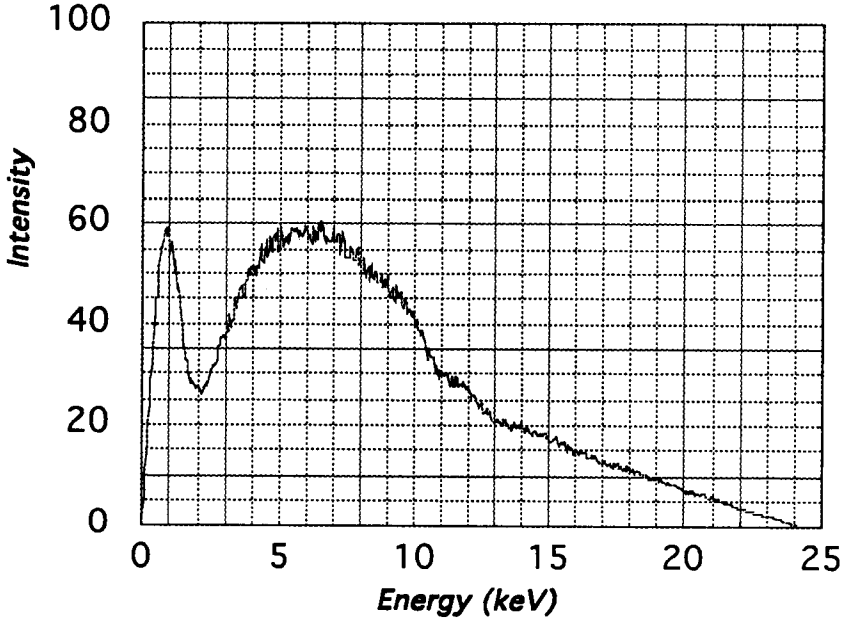

(II)

Figure 8. (continued) (i). Platinum at E0=25keV

Note that only bremsstrahlung x-ray spectrum is shown in (II)

CHAPTER 3

THE APPLICATION OF THE MATRIX MODEL

3-1. To Examine BSE, SE Signals on an Edge Inclination Topography

Figure 9 shows the diffusion matrix calculation of BSE and SE signals on a silicon structure (curve c), which is assumed to be observed at 2.0keV beam energy, an edge inclined at 40° to the horizontal and rising to height of R, R/2, and R/5, where R is the Bethe electron range, which for silicon at 2 keV is 1000Å. The profiles show the backscattered signals, computed for steps spaced by 50Å, simulated by the diffusion matrix method for the two detectors A and B. One collects all of the backscattered electrons moving to the right (+x) direction, while the other collects all of the electrons moving in the left (-x) direction. The form of each of these signals is in excellent agreement both with experimental data and with conventional Monte Carlo computations. It is noted that changing the height of the structure not only changes the width of the edge portions of the profile, as would of course be expected from the geometry, but also alters the shape of the line profile. This demonstrates that measurement algorithms which rely on a specified shape of a profile for their accuracy will also be sensitive to the absolute height of the structure.

Figure 10 shows an application to a silicon structure with edge inclinations of nominally 80° to the horizontal. The structure is 1.0μm wide at the base and 1.0μm high. The comparison of BSE and SE signals by matrix method to that by conventional Monte Carlo simulation is shown in figure 10.

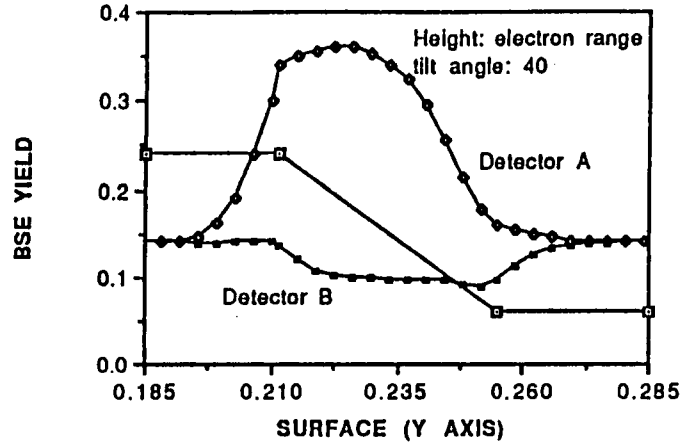

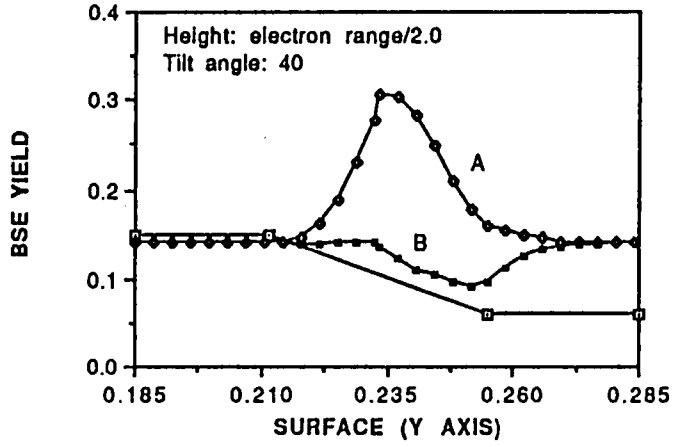

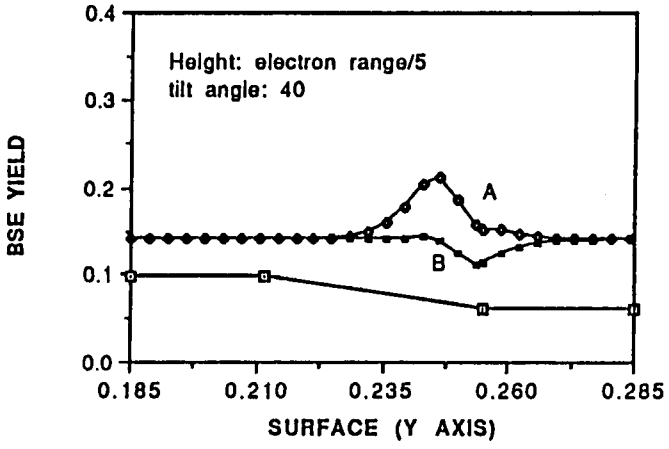

Figure 9. Comparison of BSE signals from detector A and B for silicon specimen at 2.0keV. The edge height is R, R/2, and R/5 respectively, and the tilt angle is 40 degrees.

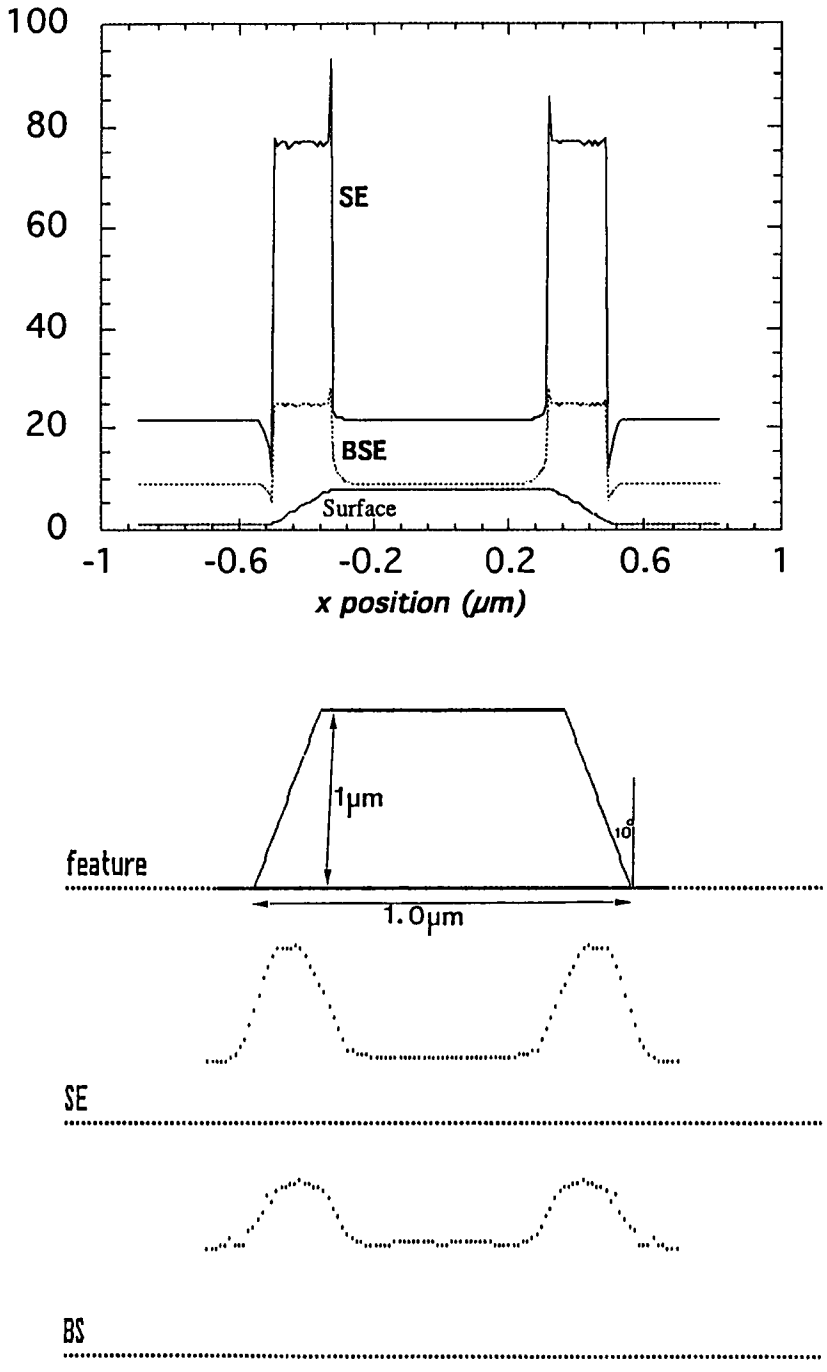

Figure 10. Comparison of BSE and SE signals by matrix model to that by Monte Carlo simulation on a silicon structure. The sample is 1.0μm wide, 1.0μm high and with wall at 80 degrees to the horizontal, and observed at 2.0keV.

3-2. EDS Spectrum for Rough Materials

For aluminum micro-spherical particles with radius R/5, R/4, R respectively, where R is the Bethe range which is about 4μm for Al at E0=20keV, the diffusion matrix is applied to approximate the distribution of the energy dispersive spectrum and the result is shown in figure 11. The results of these calculations suggest that as the size of the sample is increased, the intensity of the bremsstrahlung radiation is increased, and the bremsstrahlung energy with maximum intensity is also increased with radius.

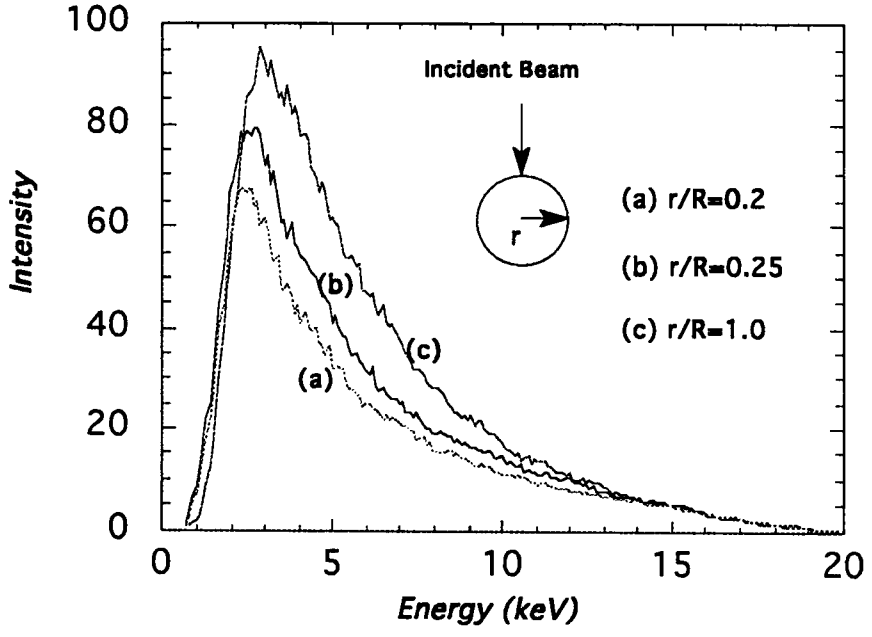

Figure 11. Diffusion matrix calculation of bremsstrahlung x-ray for a round Al particle at 20 keV. The radius of the sample is (a) R/5, (b) R/4, (c) R, where R is the Bethe range.

The application of the matrix method to a rough surface is shown in figure 12. Here, the calculation has been performed at three specific incident points on a wave-shaped topography specimen. Curve (a) refers to the electron impact at the top of the rough surface, and (c) corresponds to the incidence at the bottom of the surface. It is possible to consider all the rough surface as a kind of wave shaped profile by a mathematical transformation, and such an approach can work on an irregular rough surface.

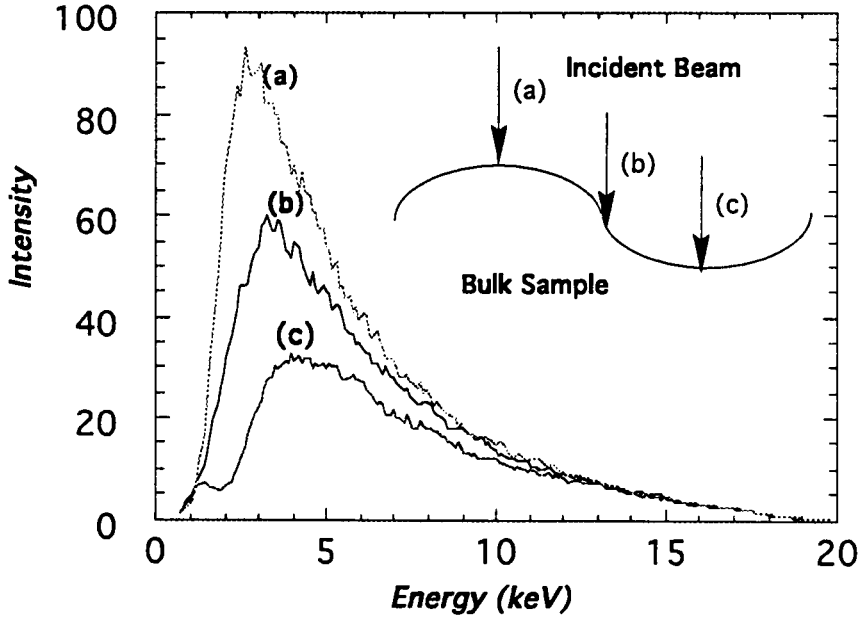

Figure 12. Diffusion matrix calculation of bremsstrahlung x-ray on a wave shaped surface of Al specimen at 20keV. The incident point is on the (a) top, (b) middle and (c)valley of the rough surface.

3.-3. The Use of the Background Radiation in Electron Probe Micro-analysis of Bulk Samples

It has been described by Nockolds (1988) that if the background radiation is a well defined function of the average atomic number of a bulk material, then the background can be used to compensate for changes in the beam exposure in electron probe analysis. The log plot of the integral of background radiation to atomic number (from Carbon to Platinum) is shown in figure 13, and gives almost a linear relation. The proportional relation between B and Z suggests that the possibility of the use of B as a measure of the beam exposure for an analysis.

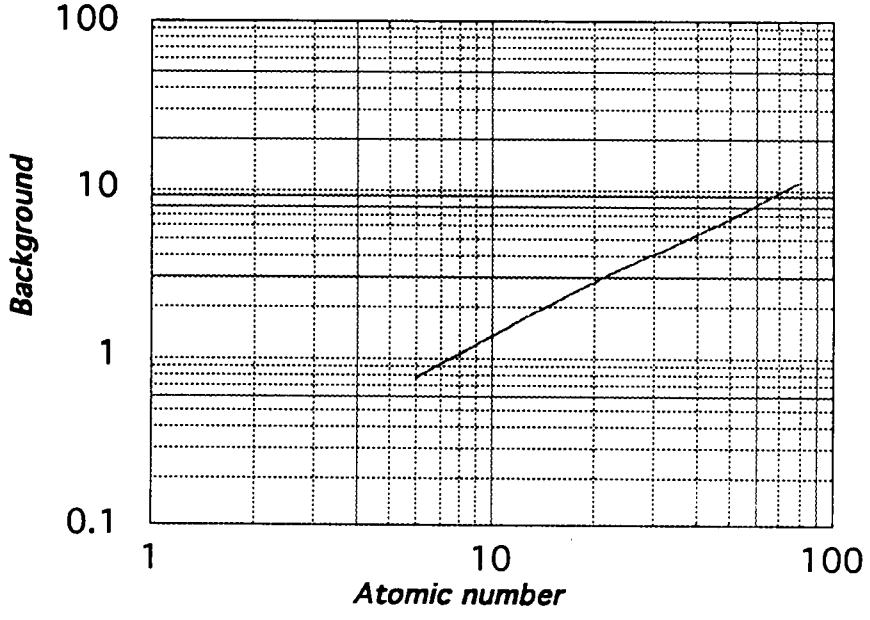

Figure 13. Log plot of the integral of background radiation to atomic number

3-4. Properties of Characteristic-to-bremsstrahlung Ratios

It has been observed that to a first approximation, the P/B ratio is relatively insensitive to the size or shape of the specimen, and to the surface roughness. Since the stopping power for bremsstrahlung production were the same as for characteristic x-rays of the same energy, the loss of radiation from through penetration or backscattered would reduce the production of both types of x-rays by the same amount, the depth distribution would be the same, and the absorption of both kinds of x-rays would be the same. Consequently, the ratio of characteristic to bremsstrahlung (peak-to-background or P/B) would not vary, for the usually minor effect of secondary fluorescence. It is instructive to confirm the practical usage of a diffusion matrix model to predict the x-ray signals on a concave surface by evaluating the P/B ratio.

CHAPTER 4

THE FURTHER APPLICATION OF THE MATRIX MODEL TO HETEROGENEOUS SPECIMEN

4-1. EDS Spectrum Simulation for a System with More Than One Component

For a system with more than one component, usually we can use the average physical parameters, which are evaluated by $\Sigma c_i p_i$, where c_i is the atomic fraction of component i, and p_i is any specific physical parameters of component i, to simulate the electron scattering behavior by assuming all the components are uniformly distributed. However, it requires a fresh Monte Carlo computation for any multi-component system. An alternative simulation is approached in this paper by using the known diffusion matrix for any single component mentioned in the early chapters. We only need to convert the accounts from any grid of each component by multiplying its atomic fraction, and then sum the contribution from each composition.

The EDS spectrum of a 50% Fe-Ni alloy is examined here. For such an alloy system, the intensity of x-ray signal of each component is calculated by multiplying its atomic fraction to all its matrix array, which is a known matrix for either pure Fe or Ni under specified experimental condition. By considering the mass absorption respectively, the emitted x-ray intensity from every component is accumulated, so that the total x-ray signals is simulated. The agreement of the computed data to the experimental data is shown in figure 14.

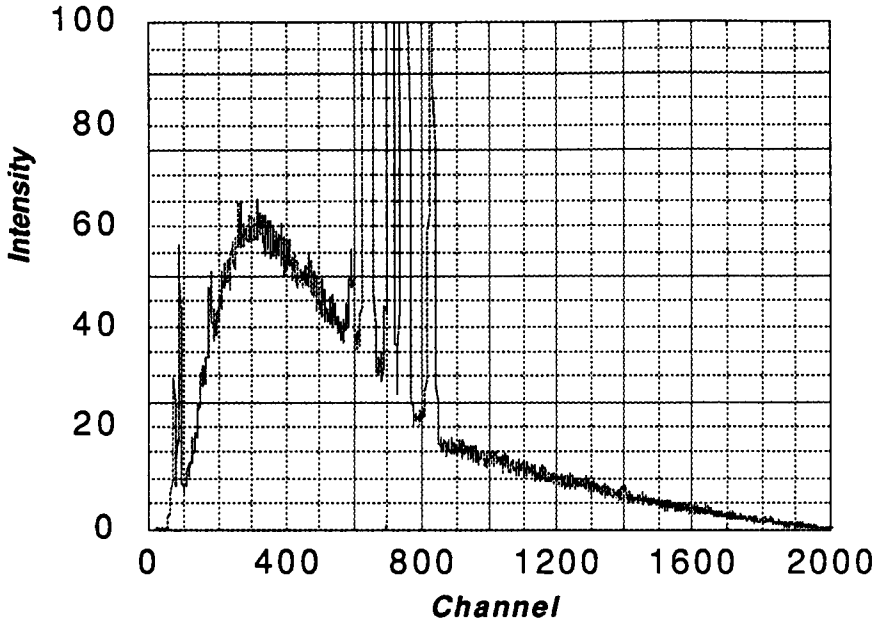

(a)

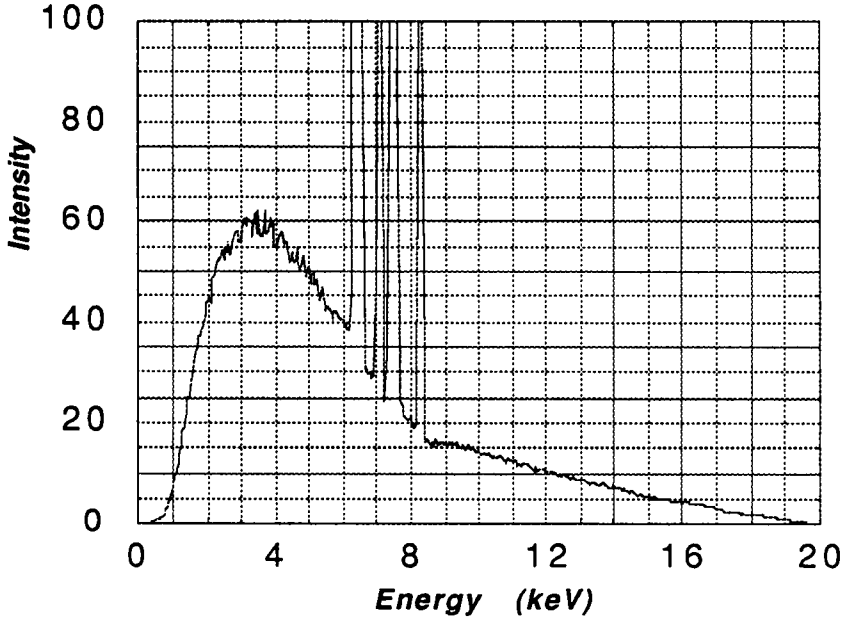

(b)

Figure 14. EDS spectrum of Fe-Ni alloy at E0=20keV (a) from the experimental data b) from the calculation by diffusion matrix method

4-2. EDS Spectrum Evaluation for a Multi-layer Sample

For a known thickness multi-layer sample, we proceed on a layer by layer calculation. In principle, the total x-ray signal is calculated by summing the contribution from each layer in the scattering range.

First of all, we should determine N1, the array number of the matrix to be considered in the first layer, by dividing the thickness of the layer to the grid length of this component. For the first layer, all the grids $BR(z_i,x_j,E_b)$ in the range of $1 < i < N1$, $1 < j < 20$ are added as this layer's contribution. Moreover, the average energy as the electron leaves the edge of the first layer should be calculated from another matrix that contains the average energy at any depth of the pure specimen. Second of all, once an electron goes into another medium, the previous scattering history is transformed to be equivalent to that which happens in the new medium, so all of the electron scattering events occurred before entering a second layer can be regarded as those happening in it equivalently. By using the edge energy, we can figure out the equivalent depth that the electron might have traveled in the second layer, which gives us the starting x-ray generation array number N1' of the second matrix. On calculating $\Delta N2$, which is the ratio of the thickness of the second layer to the grid length of that component, we add all the grids $BR(z_i,x_j,E_b)$ in the range of $N1' < j < (N1'+\Delta N2)$, $1 < i < 20$ as the contribution from the second layer. Such a procedure is then repeated for any layer inside the interaction range. The schematic illustration is shown in figure 15. EDS spectrum is then evaluated by adding the characteristic x-ray generation.

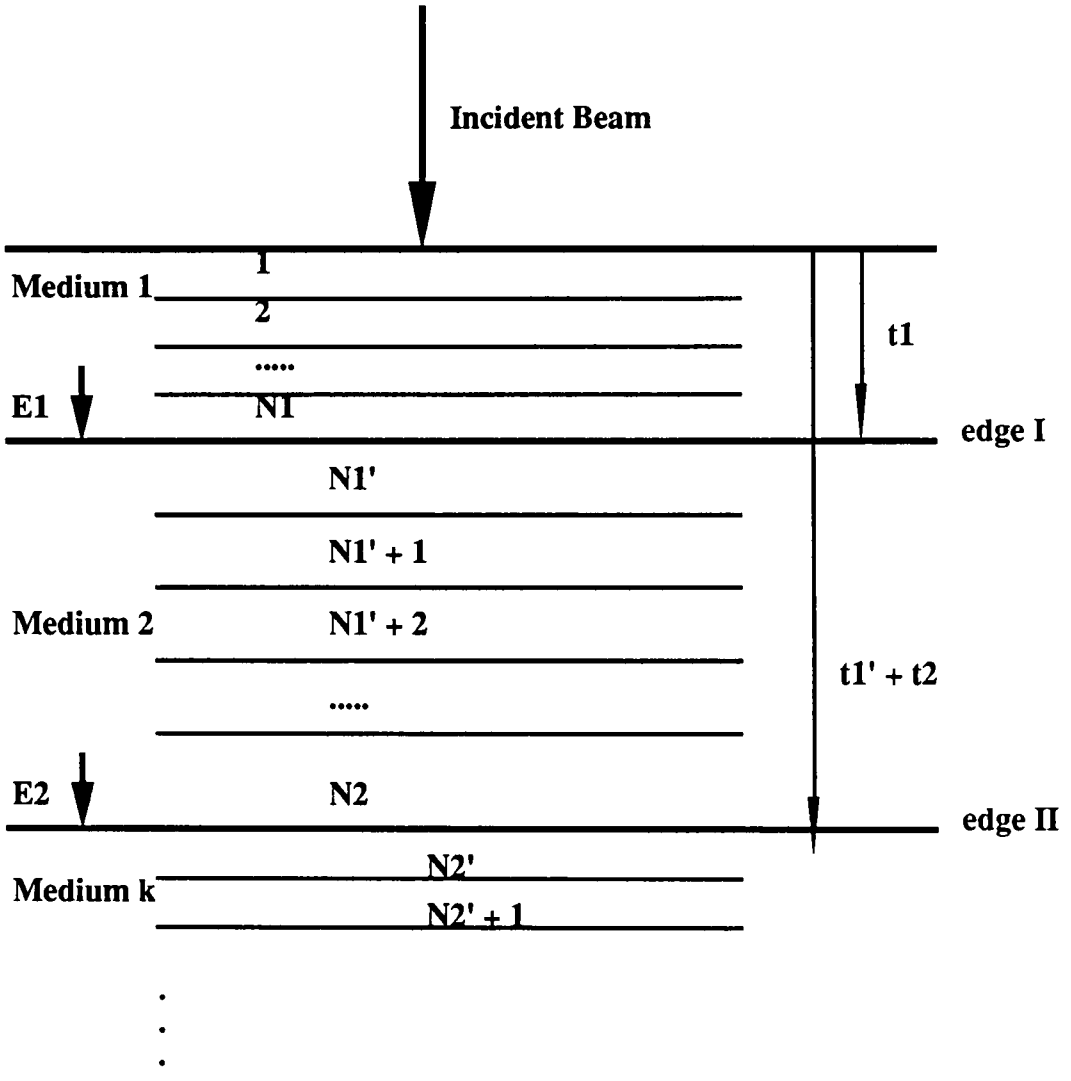

Figure 15. Schematic illustration of the application of matrix method to multi-layer film specimen. Assume the average escaping energy at edge I from medium 1 equals to the bombardment energy to the medium 2, we can estimate value N1', the starting matrix number of medium 2, from N1, which is determined by t1 and step length of medium 1.

A Cu/Cr two-layer sample is examined here. The surface of a Chromium bulk specimen was polished and then a thin copper film evaporated on it. The thickness of the copper film was determined simply by the weight of the evaporated copper divided by its density and surface area. The specimen was measured at E0=20keV by SEM-800 to compare with the calculation by matrix method. The results are shown in figure 16.

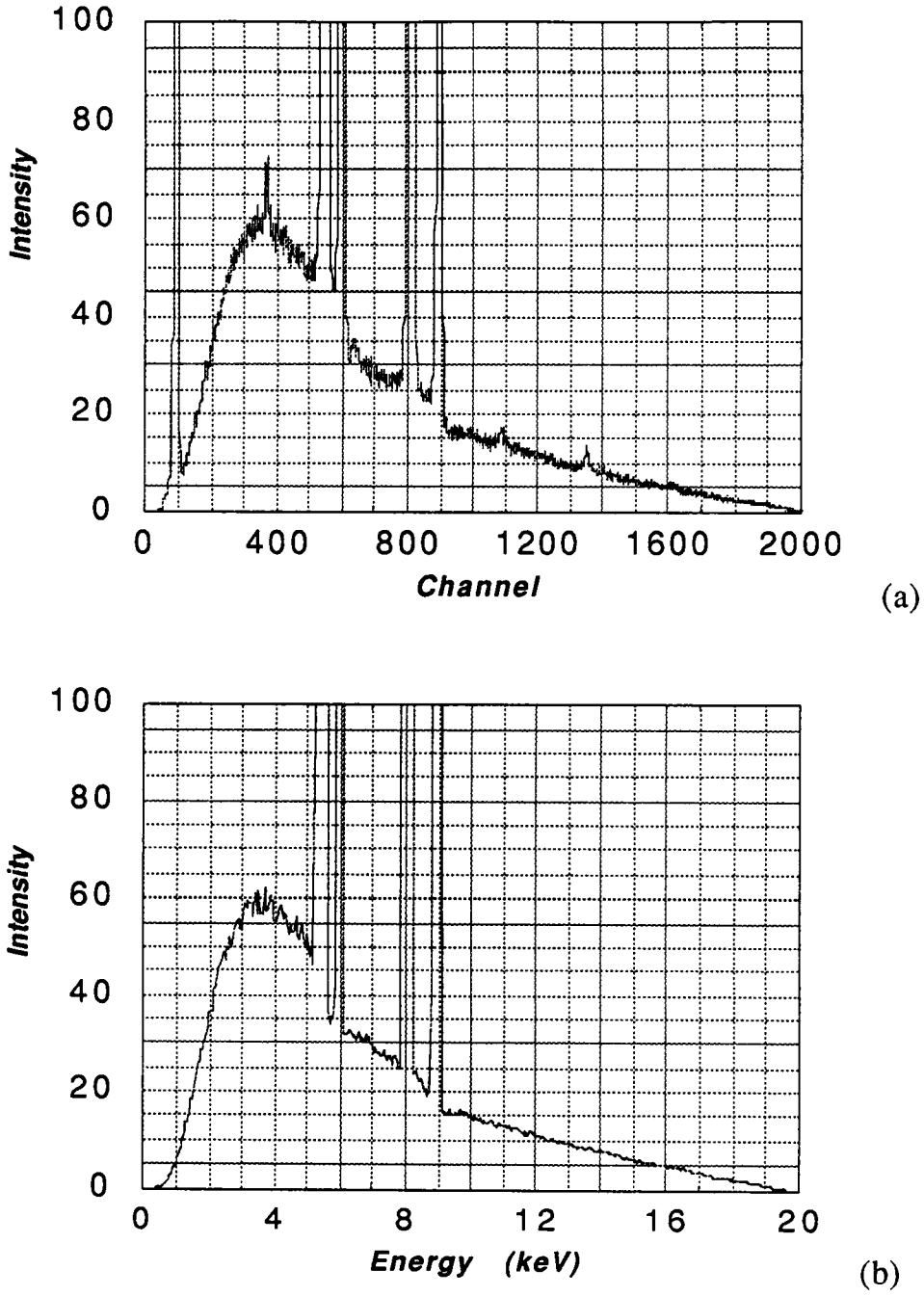

Figure 16. EDS spectrum of Cu-Cr two-layer sample with t_{Cu}= 5208Å at E0=20keV. (a) measured at SEM-800, (b) calculated by diffusion matrix method.

CHAPTER 5

SUMMARY

5-1. Discussion

The results presented above show that the diffusion matrix model is capable of producing accurate representations of BSE, SE signals, and x-ray spectrum of arbitrary geometry in a short time compared to direct Monte Carlo calculation. The method has the advantage that it can model micro-particle and arbitrary geometry specimen in a fraction of time without the need of a new set of a Monte Carlo simulation. It is possible to examine the effects of changing the positions and properties of the detectors, the tilt of the incident beam for BSE, SE simulation, and also to determine the EDS spectrum for heterogeneous specimens, multi-layer film samples.

The diffusion matrix method does, however, still have some drawbacks compared to the Monte Carlo approach.

1) Since the matrix is established by imaging the electron interacting with solid in all space until it ultimately loses its energy, the BSE, SE and x-ray signals could be all overestimated in the real geometry calculation because those escaping electrons (backscattered and secondary electrons) are not considered.

2) A matrix is only applicable to one material at specific incident energy. Thus generalizing the new BSE, SE, x-ray signals from a single material to several different materials is not straightforward. However, because changing from one material to another

mainly causes a change in the effective scale of the matrix it is obvious in principle what needs to be done to remove this limitation, i.e., a further study is expected to show BSE, SE and X-ray signals on an arbitrary topography for a series materials by using one matrix of a typical material and its relative value of Bethe range to the other materials.

Some further approaches of the matrix model and its application:

1). To develop an empirical equation which is able to generate the matrix element from some basic physical parameters of any material, and then rapidly predict the appropriate BSE, SE, X-ray signal of any known component specimen.

2). To evaluate the geometry profile of the known sample by comparing the computer simulation and experimental signal.

3). To compute EDS spectrum for a material A with several micro-meters sized inclusions B, on the cross-section of a grain boundary of two materials, for a specimen with A, B, C, D etc. layers.

5-2. Conclusions

The agreement between the theoretical and measured data shows that the diffusion matrix model described in this paper is a very effective and fast way to simulate BSE, SE and x-ray signals on an arbitrary geometry profile.

LIST OF REFERENCES

LIST OF REFERENCES

[1]. Berger, M. J., Seltzer, S. M. (1964), Studies in Penetration of Charged Particles in Matter, Natl. *Acad. Sci Natl Res Council Publ* 1133, 205-228

[2]. Bethe, H. (1930), Zur Theorie des Durchganges Schneller Korpuskulerstrahlen durch Material, *Annalen de Phys. (Leipzig)*, Vol.5, 325-333.

[3]. Bishop, H. E. (1976), Monte Carlo Simulations, in *Use of Monte Carlo Calculations in Electron Probe Microanalysis and Scanning Electron Microscope,* ed K. F. J. Heinrich et al. (NBS Special Publication 460), 5-15.

[4]. Burden, R. L., Faires J. D. (1989), *Numerical Analysis*, 4th ed. 126-138, PWS-KENT Publishing Company.

[5]. Burhop, E. H. S. (1955), Le Rendement de Fluorescence, *J. Phys. Radium* Vol.16: 625

[6]. Casnati, E., Tartari A. and Barald C. (1982), An empirical approach to K-shell ionization cross-section by electrons, *J. Phys. B:* At. Mol. Phys. Vol.15 155-167

[7]. Colby, J. W., (1968), Quantitative microprobe analysis of thin insulating films, in : *Advances in X-ray Analysis,* Vol.11, Eds. J. Newkirk, G. Mallett and H. Pfeiffer (Plenum, New York) p. 287

[8]. Curgenven, L., Duncumb, P. (1971), Simulation of Electron Trajectories in a Solid Target by a Simple Monte Carlo Technique, *Tube Investments Research Laboratories Report 303*

[9]. Czyzewski, Z., Joy, D. C., (1991), Calculation of Secondary Electron Production Using a Diffusion Matrix, *Scanning* Vol.13, 227

[10]. Desai, V., and Reimer, L., (1990), Calculation of the Signal of Backscattered Electron Scattering in Solids, *Scanning* Vol.12, 1

[11]. Drescher, H., Reimer, L., and Seidel, H. (1970), Ruckstreukoeffizient und Sekundarelektronenausbeute von 10-100 keV Elektronen und Beziehungen zur Rasterelektronenmikroskopie, *Z. Agnew Phys.* Vol. 29, 331

[12]. Fiori, C. E., Swyt, C. R., and Ellis, J. R. (1982), The Theoretical Characteristic to Continuum Ratio in Energy Dispersive Analysis in the Analytical Electron Microscope, *Microbeam Analysis* , ed K. F. J. Heinrich, 57

[13]. Heinrich, K.F.J. (1966), in the *Electron Microprobe*, (T. Mckinley et.al., ed.), Wiley, NY 296

[14]. Hunger, H. J., Kuchler, L. (1979), Measurements of the Electron Backscattering Coefficient for Quantitative EPMA in the Energy Range 4 to 40 keV, *Phys. stat. sol.,* (a), Vol.56, K45-K48

[15]. Joy, D. C. (1991), An Introduction to Monte Carlo Simulations, *Scanning Microscopy*, Vol.5, No.2, 329-337

[16]. Joy, D.C, Luo, S. (1989), An Empirical Stopping Power Expression for Low Energy Electrons, *Scanning* Vol.11, 176

[17]. Joy, D. C. et al., (1986), *Principles of analytical electron microscopy,* Plenum Press, 413-441

[18]. Kirkpatrick, P. and Wiedmann, L. (1945), Theoretical Continuous X-ray Energy and Polarization, Physical Review, Vol.67, No.11 & 12, 321

[19]. Love, G, Cox M. G.C., Scott V. D. (1977), A Simple Monte Carlo Method for Simulation Electron-solid Interactions and its Application to Electron Probe Microanalysis, *J. Phys. D: Appl. Phys.,* Vol.10, 7-23

[20]. Motz, J. W. and Placious, R. C. (1958), Bremsstrahlung Cross-section Measurements for 50-keV Electrons, *Physical Review* , Vol.109, No.2, 235

[21]. Newbury D. E., Yakowitz H., Myklebust R. L.(1976), The NBS Monte Carlo program, in *Use of Monte Carlo calculations in Electron Probe Microanalysis and Scanning Electron Microscopy,* ed K F J Heinrich et al. (NBS Special Publication 460), 151-164

[22]. Nockolds, C. E., and Griffin B. J.(1988), The Use of the Background Radiation in Electron Probe Analysis of Bulk Samples, *Proc. IVth Asia-Pacific Conference and Workshop on Electron Microscopy*, Bangkok

[23]. Russ J. C. (1984), *Fundamentals of energy dispersive x-ray analysis,* Butterworths & Co(Ltd.), 72

[24]. Schreiber, T. P. and Mims, A. M. (1981), A Quantitative X-ray Microanalysis Thin Film Method Using K, L, and M-lines, *Ultramicroscopy* , 6 323-334

[25]. Sommerfeld, A. (1931) , Uber die Beugung und Bremsung der elektronen, *Ann. Phys.* 11,257

[26]. Statham, P. J. (1976), The Generation, Absorption and Anisotropy of Thick-target Bremsstrahlung and Implications for Quantitative Energy Dispersive Analysis, *X-ray Spectrometry,* Vol. 5, 154

[27]. Wang, X. and Joy D. C. (1991), A New High-speed Simulation Method for Electron-beam Critical Dimension Metrology Profile Modeling, *J.Vac.Sci.Technol. B* Vol.9, No.6, Nov/Dec

APPENDIX

```
C     THE DEVELOPMENT OF THE DIFFUSION MATRIX
C     June, 1992

C     The diffusion matrix is created by using Monte Carlo simulation in this program.
C     Both backscattered and secondary electron yield is stored in the matrix BSSE(zj,xi,ak,bl),
C     where bl =1 or 2, refers to BSE or SE signals respectively.
C     EDS spectrum  is stored in the matrix PHI(zj,xi,Ek,gl), where gl =1 to 4,  refers to
C     bremsstrahlung, K,L, and M shell x-ray generation respectively.

      REAL*8 DUM,EI,FI
      CHARACTER*6 FNAME,FNAMB,FNAMX
      CHARACTER*2 FN(3),EL,FB(3),FX(3)
      EQUIVALENCE(FN,FNAME),(FB,FNAMB),(FX,FNAMX)
      DATA FN/'EL','.D','AT'/
      DATA FB/'EL','.B','SE'/
      DATA FX/'EL','.R','AY'/

      COMMON/RAND/EI,FI,DUM
      COMMON/BEAM/E(51)
      COMMON/MAT/ZA,RU,A,EJ,SS,DR
      COMMON/ACOOD/X0,Y0,Z0,X1,Y1,Z1,CX,CY,CZ,CA,CB,CC,SP,CP,GA
      COMMON/GRID/PHI(40,20,30,4),BSSE(40,20,36,2),EC(3),NOE(3)

C     Constants and initial values to generate random numbers

      PI=ATAN(1.0)*4.0
      EI=67101323.0
      FI=8192.0

C     Input some physical parameters, such as atomic number, atomic weight, density,
C     incident energy, electron trajectories, detector position

      WRITE(*,*)'WHICH ELEMENT?'
      READ(*,555)EL
      FN(1)=EL
      FX(1)=EL
      FB(1)=EL
555   FORMAT(A2)

      WRITE(*,*)'PRIMARY ENERGY?'
      READ(*,*)E0
      WRITE(*,*)'NUMBER OF TRAJECTORIES?'
      READ(*,*)NN
      WRITE(*,*)'TILT ANGLE OF INCIDENCE?'
      READ(*,*)A0
      WRITE(*,*)'TAKE OFF ANGLE IN DEGREE?'
      READ(*,*)TOA
      TOA=TOA*PI/180.0

      OPEN(5,FILE=FNAME,STATUS='OLD')
      OPEN(8,FILE=FNAMB,STATUS='NEW')
      OPEN(10,FILE=FNAMX,STATUS='NEW')
      READ(5,10)ZA,A,RU
10    FORMAT(3F7.3)
```

```
      READ(5,11)(EC(I),I=1,3)
11    FORMAT(3F7.3)

C     Set electron numbers in K, L, M shell

      NOE(1)=2
      NOE(2)=8
      NOE(3)=18

      DO I=1,3
      IF (EC(I).EQ.0.0)THEN
      NT=I
      GOTO 12
      END IF
      END DO
      NT=3

C     Set matrix BSSE and PHI zero at the beginning of the simulation

12    DO I=1,40
        DO J=1,20
          DO K1=1,30
            DO K2=1,NT+1
            PHI(I,J,K1,K2)=0.0
            END DO
          END DO
        END DO
      END DO


      DO I=1,40
        DO J=1,20
          DO K1=1,36
            DO K2=1,2
            BSSE(I,J,K1,K2)=0.0
            END DO
          END DO
        END DO
      END DO

C     Find the screened Rutherford scattering parameter b
C     First get the Love-Scott-Hunger Kuchler scattering factor

      HKM=0.1382-0.9211/SQRT(ZA)
      DUM=ALOG(ZA)
      HKC=0.1904-0.2235*DUM+0.1292*DUM*DUM-0.01491*(ALOG(ZA))**3.0

      HKBS=HKC*E0**HKM

      B=0.016697+0.55108*HKBS-0.96777*HKBS*HKBS+1.8846*HKBS**3.0

C     To calculate electron Bethe range
C     To get the step length, which is assumed to be 50 equal steps by plural model

      CALL ERANGE(E0,RANGE)
```

```
      STEP=RANGE/50.0

C     Output all the input parameters on screen

      WRITE(*,22)E0,A0
22    FORMAT(1X,'E0=',F10.2,2X,'A0=',F10.2)
      WRITE(*,24)NN
24    FORMAT(1X,'NN=',I8)
      WRITE(*,28)ZA,A,RU
28    FORMAT(1X,'ZA=',F10.4,2X,'A=',F10.4,2X,'RU=',F10.4)
      WRITE(*,32)EJ,EC(1),EC(2),EC(3)
32    FORMAT(1X,'EJ=',F10.4,'EC',3F10.4)
      WRITE(*,*)' '

C     To calculte the energy loss by modified Bethe equation

      CALL ELOSS(E0)

      WRITE(*,50)(E(I),I=1,50)
50    FORMAT(1X,5F10.4)
      WRITE(*,*)' '

C     SIMULATION STARTING

      KPN=1
      DO 100 I=1,NN

C     To initialize the coordinates and directional cosine for every incident electron

      DUM=DBLE(I)/(NN+1.0)*EI
      X0=0.0
      Y0=0.0
      Z0=0.0
      AX0=0.0

      CX=0.0
      CY=SIN(A0/57.4)
      CZ=COS(A0/57.4)

      IX0=1
      IZ0=21

C     Print current trajectory number every 100 simulation

      KPP=KPN
      KPN=INT(FLOAT(I)/100.0)

      IF (KPP.EQ.KPN) GOTO 7
      WRITE(*,*)'NUMBER OF CURRENT TRAJECTORY=',I

C     To trace any electron that travels in the specimen till its energy drops to a
C     min. value

7     DO 200 K=1,50
      EN=E(K)
```

```
      CALL SCTTER(PI,B,E0,EN)
      CALL TRIG(STEP)

C     The interaction volume is divided into the grids of equal size DR=R/20
C     Due to the symmetry of the electron trajectory, those electrons that travels at
C     negative x side are added to the matrix by their absolute value

      AX1=ABS(X1)

      IX1=INT(AX1/DR+1.0)
      IZ1=INT(Z1/DR+21.0)

C     If the electron passes through the boundary of positive and negative x side,
C     these two sides should be considered separately.

      IF(X0*X1.LT.0.0)THEN
      AXX1=AX1
      IXX1=IX1
      YY1=Y1
      ZZ1=Z1
      IZZ1=IZ1

      AX1=0.0
      IX1=1

      Z1=Z0+(ZZ1-Z0)*(-X0)/(X1-X0)
      Y1=Y0+(YY1-Y0)*(-X0)/(X1-X0)
      IZ1=INT(Z1/DR+21.0)

      CALL GRID(AX0,AX1,IX0,IZ0,IX1,IZ1,PI,E0,EN,STEP,NT,TOA)

      AX0=0.0
      IX0=1
      Y0=Y1
      Z0=Z1
      IZ0=IZ1

      AX1=AXX1
      IX1=IXX1
      Y1=YY1
      Z1=ZZ1
      IZ1=IZZ1

      CALL GRID(AX0,AX1,IX0,IZ0,IX1,IZ1,PI,E0,EN,STEP,NT,TOA)
      GO TO 300
      ENDIF

C     To add contribution of BSE, SE, or bremsstrahlung, and characteristic x-ray generation
C     to the grids which are passed by the BSE or x-ray photon respectively

      CALL GRID(AX0,AX1,IX0,IZ0,IX1,IZ1,PI,E0,EN,STEP,NT,TOA)

300   CX=CA
      CY=CB
      CZ=CC
```

```
      X0=X1
      Y0=Y1
      Z0=Z1

      AX0=AX1
      IX0=IX1
      IZ0=IZ1

200   CONTINUE
100   CONTINUE

C     Output matrix BSSE and PHI in unit 8 and 10 seperately, where DR=range/20

      WRITE(10,75)DR
75    FORMAT(1X,E12.4)
      NT=NT+1
      WRITE(10,76)NT
76    FORMAT(1X,I2)
      DO I=1,40
        DO J=1,20
          DO K2=1,NT
          WRITE(10,80)(PHI(I,J,K1,K2),K1=1,30)
80          FORMAT(1X,6E10.2)
          END DO
        END DO
      END DO

      WRITE(8,75)DR
      DO I=1,40
        DO J=1,20
          DO K2=1,2
          WRITE(8,80)(BSSE(I,J,K1,K2),K1=1,36)
          END DO
        END DO
      END DO

      STOP
      END


C     ************************************************************************
C     *                                                                      *
C     *  SUBROUTINE AND FUNCTION USED IN MONTE CARLO ROUTINES                *
C     *                                                                      *
C     ************************************************************************

      SUBROUTINE RAND(RAN)

C     Random number generator

      REAL*8 DUM,EI,FI
      INTEGER*4 KM
      COMMON/RAND/EI,FI,DUM
      KM=INT(DUM/DBLE(EI)*FI)
      DUM=DUM*FI-KM*EI
```

```
      RAN=DBLE(DUM/EI)
      RETURN
      END


      SUBROUTINE ERANGE(XEN,RANGE)

C     This routine calculates the range in cm for an incident energy XEN
C     by the modified Bethe equation

      COMMON/MAT/ZA,RU,A,EJ,SS,DR

C     Get the mean ionization potential from usual Berger and Selzer data

      EJ=((9.76*ZA)+(58.5/(ZA**0.19)))*1.0E-3

C     Now find the CSDA-range by numerical integration

      FS=0.0

      DO M=1,21
      EN=(XEN/20.0)*FLOAT(M-1)
      F=1.0/BETHE(EN)

      VAL=2.0
      IF(MOD(M,2).EQ.0) VAL=4.0
      IF (M.EQ.1) VAL=1.0
      IF(M.EQ.21) VAL=1.0
      FS=FS+VAL*F
      END DO

C     End of the integration

      RCON=FS*XEN/60.0
      SS=RCON/50.0
      RANGE=SS*5.0E5/RU

C     Print out for diagnostics

      RANGE=RANGE*1.0E-4
      WRITE(*,150)RANGE
150   FORMAT('RANGE IS',F12.8,' cm')

      DR=RANGE/20.0
      RETURN
      END


      FUNCTION BETHE(EN)

C     The modified Bethe energy loss equation

      COMMON/MAT/ZA,RU,A,EJ,SS,DR

      IF(EN.LT.0.05) EN=0.05
```

```
      BETHE=7.85E4*ZA*(LOG(1.166*(EN+0.85*EJ)/EJ))/(A*EN)

      RETURN
      END


      SUBROUTINE ELOSS(XEN)

C     Computes a 50 step energy profile assuming the modified Bethe
C     energy loss relation

      COMMON/BEAM/E(51)
      COMMON/MAT/ZA,RU,A,EJ,SS,DR

      E(1)=XEN

C     Iterate to get the profile

      DO M=2,51

      A1=SS*BETHE(E(M-1))
      A1T=A1/2.

      A2=SS*BETHE(E(M-1)-A1T)
      A2T=A2/2.

      A3=SS*BETHE(E(M-1)-A2T)

      A4=SS*BETHE(E(M-1)-A3)

      E(M)=E(M-1)-((A1+2.0*A2+2.0*A3+A4)/6.)

      END DO

C     Set the last value to zero and smooth the profile

      E(51)=0.0

      DO M=2,50
      E(M)=(E(M)+E(M+1))/2.0
      END DO

      RETURN
      END


      SUBROUTINE  SCTTER(PI,B,E0,EN)

C     Computes the scattering using Rutherford screened cross-section

      COMMON/ACOOD/X0,Y0,Z0,X1,Y1,Z1,CX,CY,CZ,CA,CB,CC,SP,CP,GA
      REAL*8 DUM,EI,FI
      COMMON/RAND/EI,FI,DUM
```

```
      CALL RAND(RAN)
      RR=SNGL(RAN)
C     First get the Love-Scott-Hunger Kuchier scattering factor
      TH=B*E0/EN*(1.0/SQRT(RR)-1.0)
C     TH is the scattering angle cot(B/2)
      SP=(TH+TH)/(1.0+(TH*TH))
      CP=(1.0-(TH*TH))/(1.0+(TH*TH))
C     And find the azimuthal angle
      CALL RAND(RAN)
      RR=SNGL(RAN)
      GA=2.0*PI*RR
      RETURN
      END

      SUBROUTINE TRIG(ST)
C     Computes the new coordinates and the scattering angles, the step length
      COMMON/ACOOD/X0,Y0,Z0,X1,Y1,Z1,CX,CY,CZ,CA,CB,CC,SP,CP,GA
      IF (CZ.EQ.0.0) CZ=0.0001
      ANM=(-CX/CZ)
      ANN=1.0/SQRT(1.0+(ANM*ANM))
      V1=ANN*SP
      V2=ANN*ANM*SP
      V3=COS(GA)
      V4=SIN(GA)
C     Find the new direction cosines
      CA=(CX*CP)+(V1*V3)+(CY*V2*V4)
      CB=(CY*CP)+(V4*(CZ*V1-CX*V2))
      CC=(CZ*CP)+(V2*V3)-(CY*V1*V4)
C     And get the new coordinates
      X1=X0+ST*CA
      Y1=Y0+ST*CB
      Z1=Z0+ST*CC
      RETURN
      END

      SUBROUTINE GRID(AX0,AX1,IX0,IZ0,IX1,IZ1,PI,E0,EN,STEP,NT,TOA)
C     To compute the contribution to matrix BSSE and PHI for any single
```

```
C       step during the interaction of the electron and solids

        REAL*8 DX(4),DZ(4),DY(4),DEL(4)
        INTEGER*4 IDD(3,2)

        COMMON/BEAM/E(51)
        COMMON/MAT/ZA,RU,A,EJ,SS,DR
        COMMON/ACOOD/X0,Y0,Z0,X1,Y1,Z1,CX,CY,CZ,CA,CB,CC,SP,CP,GA
        COMMON/GRID/PHI(40,20,30,4),BSSE(40,20,36,2),EC(3),NOE(3)

C       Since the step is defined as R/50, and the grids size is R/20, it is considered that electron can pass
C       at most three grids at any single step. In the routine, the number of the cells that the electron
C       travels at one step is set to be NG.

        IXX=ABS(IX1-IX0)
        IZZ=ABS(IZ1-IZ0)
        NIN=IXX+IZZ

C       To find the coordinates of the intersection between the grids and BSE or x-ray photons
C       and then determine the block numbers for grids

        IF(NIN.EQ.0)THEN
        NG=1
        DX(1)=AX0
        DX(2)=AX1

        DY(1)=Y0
        DY(2)=Y1

        DZ(1)=Z0
        DZ(2)=Z1

        IDD(1,1)=IX1
        IDD(1,2)=IZ1

        ELSE IF (NIN.EQ.1) THEN

        NG=2
        DX(1)=AX0
        DY(1)=Y0
        DZ(1)=Z0

        IDD(1,1)=IX0
        IDD(1,2)=IZ0

        DX(3)=AX1
        DY(3)=Y1
        DZ(3)=Z1

        IXX=IX1-IX0

        IF(IXX)10,20,30
20      IF(Z1.GE.Z0) THEN
        ZC=DR*FLOAT(IZ0-20)
        ELSE
```

```
      ZC=DR*FLOAT(IZ1-20)
      END IF

      XC=AX0+(AX1-AX0)*(ZC-Z0)/(Z1-Z0)
      YC=Y0+(Y1-Y0)*(ZC-Z0)/(Z1-Z0)
      GO TO 40

10    XC=DR*FLOAT(IX1)
      ZC=Z0+(Z1-Z0)*(XC-AX0)/(AX1-AX0)
      YC=Y0+(Y1-Y0)*(XC-AX0)/(AX1-AX0)
      GO TO 40

30    XC=DR*FLOAT(IX0)
      ZC=Z0+(Z1-Z0)*(XC-AX0)/(AX1-AX0)
      YC=Y0+(Y1-Y0)*(XC-AX0)/(AX1-AX0)

40    DX(2)=XC
      DY(2)=YC
      DZ(2)=ZC

      IDD(2,1)=IX1
      IDD(2,2)=IZ1

      ELSE IF (NIN.EQ.2) THEN

      NG=3

      IF(IX1.GT.IX0)THEN
      RATIO=1.0
      DX(2)=FLOAT(IX0)*DR
      ELSE
      RATIO=-1.0
      DX(2)=FLOAT(IX1)*DR
      END IF

      DZ(2)=(Z1-Z0)/(AX1-AX0)*(DX(2)-AX1)+Z1
      DY(2)=(Y1-Y0)/(AX1-AX0)*(DX(2)-AX1)+Y1

      IF(IZ1.GE.IZ0)THEN
      DZ(3)=FLOAT(IZ0-20)*DR
      ELSE
      DZ(3)=FLOAT(IZ1-20)*DR
      END IF

      DX(3)=AX0+(AX1-AX0)*(DZ(3)-Z0)/(Z1-Z0)
      DY(3)=Y0+(Y1-Y0)*(DZ(3)-Z0)/(Z1-Z0)

C     To array the observed coordinates for NG=3

      DO I=2,3
      DX(I)=RATIO*DX(I)
      END DO

      IF (DX(2)-DX(3)) 50,60,70
70    AS=DX(2)
```

```
      BS=DY(2)
      CS=DZ(2)

      DX(2)=DX(3)
      DY(2)=DY(3)
      DZ(2)=DZ(3)

      DX(3)=AS
      DY(3)=BS
      DZ(3)=CS

      GOTO 50
60    NG=NG-1

50    DO  I=2,3
      DX(I)=RATIO*DX(I)
      END DO

      DX(1)=AX0
      DX(NG+1)=AX1
      DY(1)=Y0
      DY(NG+1)=Y1
      DZ(1)=Z0
      DZ(NG+1)=Z1

C     To determine the block number of grids for NG=3

      DO  L=1,NG
      QX=(DX(L)+DX(L+1))/2.0/DR
      IDD(L,1)=INT(QX+1.0)

      QZ=(DZ(L)+DZ(L+1))/2.0/DR
      IDD(L,2)=INT(QZ+21.0)
      END DO

      END IF

C     To find the step length at each grids

      DO I=1,NG
      DEL(I)=SQRT((DX(I)-DX(I+1))*(DX(I)-DX(I+1))+(DY(I)-DY(I+1))*
     1 (DY(I)-DY(I+1))+(DZ(I)-DZ(I+1))*(DZ(I)-DZ(I+1)))
      END DO

C     To add bremsstrahlung, and characteristic x-ray generation signals to the grids
C     which are passed by BSE or x-ray photons

      DO 100 J=1,NG
      IXX=IDD(J,1)
      IZZ=IDD(J,2)

      DO M2=1,30
      PE=FLOAT(M2)*E0/30.0
      IF (EN.GT.PE) THEN
```

```
C       To get bremsstrahlung ionization cross-section by Kirkpatrick's model

        CALL FNCONT(ZA,RIX,RIY,PE,EN)

C       Bremsstrahlung radiation is assumed to be anisotropy here

        VC=SQRT(1.0-1.0/(1.0+EN/511)**2.0)
        CG=-CA*COS(TOA)-CC*SIN(TOA)
        W=(RIX*(1-CG*CG)+RIY*(1+CG*CG))
     1  /(1-VC*CG)**2.0/PE
        CONT=W*6.023E23*RU/A
        PHI(IZZ,IXX,M2,1)=PHI(IZZ,IXX,M2,1)+CONT*DEL(J)
        END IF
        END DO

C       To get characteristic ionization cross-section by Casnati's model
C       for K shell or Schreiber's model for L and M shell

        DO MN=1,NT
        M2=INT(EN*30.0/E0)
        IF (EN.GT.EC(MN))THEN

        IF(MN.EQ.1) THEN
        ECC=EC(1)

        CALL CASNATI(ECC,EN,CROSSSECTION)

        ELSE

                IF (MN.EQ.2) THEN
                BB=0.2704+0.007256*LOG(ZA)**3.0
                ELSE
                BB=11.33-2.43*LOG(ZA)
                END IF

                CROSSSECTION=6.4924E-20*FLOAT(NOE(MN))
     1                      *BB*LOG(EN/EC(MN))/EC(MN)/EN

        END IF

        CHAR=CROSSSECTION*6.023E23*RU/A
        PHI(IZZ,IXX,M2,MN+1)=PHI(IZZ,IXX,M2,MN+1)+CHAR*DEL(J)
        END IF
        END DO

C       To add BSE,SE signals to the grids which are passed by the BSE

        IF(ABS(CC).GE.1.0) CC=1.0

C       To determine the direction angle of the BSE, which is defined as the angle
C       between the positive z direction and the BSE direction

        IF(CA.GE.0.0)THEN
        THETA=ACOS(CC)*180.0/PI
        ELSE
```

```
      THETA=360.0-ACOS(CC)*180.0/PI
      END IF

      M2=INT(THETA/10.0+1.0)

C     To add BSE signals to the grids

      BSSE(IZZ,IXX,M2,1)=BSSE(IZZ,IXX,M2,1)+1.0
      SY=(E0/EN)**-0.8

C     To add SE signals to the grids excluding item sec(x) by Drescher's eq.

      BSSE(IZZ,IXX,M2,2)=BSSE(IZZ,IXX,M2,2)+SY

100   CONTINUE

      RETURN
      END


      SUBROUTINE CASNATI(EC,EN,CROSSSECTION)

C     To get K shell ionization cross-section by Casnati's model

      EJ=511.0/EC
      U=EN/EC

      R=(1.0+EN/511.0)*(1.0+EN/511.0)/(1.0+EN/1022.0)

C     RLO is the Rydberg energy 13.606 eV

      RLO=0.013606

C     A0 is the first Bohr radius = 5.292E-9 cm

      A0=5.292E-9

C     Casbati constants

      D0=-0.0318
      D1=0.316
      D2=-0.1135

      B0=10.57
      B1=-1.736
      B2=0.317

C     Now compute the various parts of the expression

      POWER1=D0+D1/U+D2/U/U
      PSI=(EC/RLO)**(POWER1)

      DUMMY=B1/U+B2/U/U
      SIGMA=B0*EXP(DUMMY)
      OVERVOLTAGE=1.0/U*ALOG(U)
```

```
C       Assume that NK=2 i.e. 2 electrons in the 1-P shell

        NK=2
        CROSSSECTION=FLOAT(NK)*A0*A0*R*(RLO/EC)*(RLO/EC)*
     1 PSI*SIGMA*OVERVOLTAGE

        RETURN
        END


        SUBROUTINE FNCONT(ZA,RIX,RIY,EM,E)

C       To get bremsstrahlung ionization cross-section by Kirkpatrick's model, where E is the current
C       energy, and EM is bremsstrahlung photon energy

        IF(E.LT.EM) GOTO 40
        VZ=E/ZA/ZA/0.2998
        RF=EM/E
        FY=1.0
        IF(VZ.LE.0.0604) GOTO 10

C       Compute K and W's fitted expression

C       To calculate RIX

        A=EXP(-0.223*VZ)-EXP(-57.0*VZ)
        B=EXP(-0.0828*VZ)-EXP(-84.9*VZ)

        AA=1.47*B-0.507*A-0.833
        BB=1.7*B-1.09*A-0.627

        X=RF-0.135
        RIX=0.252+AA*X-BB*X*X

C       To calculate RIY

        Y1=0.220*(1.0-0.390*EXP(-26.9*VZ))
        Y2=0.067+0.023/(VZ+0.75)
        Y3=-0.00259+0.00776/(VZ+0.116)

        H=1.43*Y1-2.43*Y2+Y3
        H=(-0.214*Y1+1.21*Y2-Y3)/H
        RJ=(1.0+2.0*H)*Y2-2.0*(1.0+H)*Y3
        RK=(1.0+H)*(Y3+RJ)

        RIY=ABS(-RJ+RK/(RF+H))

        RIX=RIX/VZ
        RIY=RIY/VZ
        GOTO 20

C       New expression for small V/Z2

10      X=(-1.01904+0.146014*RF-0.0501077*RF*RF)
```

```
     1 *ALOG(VZ)-1.48311+0.947484*RF-0.350014*RF*RF
          Y=(-0.882129+0.0366934*RF-0.339646*RF*RF)
     1 *ALOG(VZ)-1.04088-1.86355*RF-0.723068*RF*RF

          RIX=EXP(X)
          RIY=EXP(Y)

C         Modify formula for IY near V/V0=0

          FY=1.55-4.83*VZ
20        IF(RF.GE.0.2) GOTO 30
          D=EXP(-20.0*RF)
          RIX=RIX*(1.0-0.567*D)
          RIY=RIY*(1.0-(1.0-FY)*D)

30        RIX=RIX*1.509E-24
          RIY=RIY*1.509E-24
          RETURN

40        RIX=0.0
          RIY=0.0
          W=0.0
          RETURN
          END
```

VITA

Xinlei Wang was born in Shanghai, China on October 10, 1963. She graduated from Fuxing high school in July 1982, and then entered Fudan University, Shanghai, China. In July of 1986, a Bachelor of Science degree in Physical Chemistry was awarded to her. After being a research assistant in Shanghai Institute of Ceramics, Chinese Academia for three years and a half, she came to the University of Tennessee, Knoxville to continue her education in March 1990. She was awarded a Master of Science degree in Metallurgical Engineering in August 1992.